Article

Current and Future Habitat Suitability Models for Four Ticks of Medical Concern in Illinois, USA

Heather Lynn Kopsco[1,*], Peg Gronemeyer [2], Nohra Mateus-Pinilla [1,2], and Rebecca Lee Smith [1,3]

[1] Department of Pathobiology, College of Veterinary Medicine, University of Illinois Urbana-Champaign, Urbana, IL
[2] Illinois Natural History Survey, Prairie Research Institute, University of Illinois Urbana-Champaign, Urbana, IL
[3] Institute for Genomic Biology, University of Illinois Urbana-Champaign, Urbana, IL
* Correspondence: hkopsco@illinois.edu

Abstract: The greater U.S. Midwest is on the leading edge of tick and tick-borne disease (TBD) expansion, and tick and TBD encroachment into Illinois is occurring from both the northern and the southern regions. To assess historical and future habitat suitability of four ticks of medical concern within the state, we fit individual and mean-weighted ensemble species distribution models for *Ixodes scapularis*, *Amblyomma americanum*, *Dermacentor variabilis,* and a newly invading species, *Amblyomma maculatum* using a variety of landscape and mean climate variables for the periods of 1970-2000, 2041-2060, and 2061-2080. Ensemble models for the historical climate were consistent with known distributions of each species but predicted the habitat suitability of *A. maculatum* to be much greater throughout Illinois than what known distributions demonstrate. Proximity to wetlands and water bodies was important in predicting both *I. scapularis* and *A. americanum* presence. *A. americanum* occurrence was highly dependent on increasing forest cover, while *A. maculatum* habitat was more strongly predicted by open habitats. As the climate warmed, the expected distribution of all species became more strongly impacted by precipitation and temperature variables, particularly mean temperature of the wettest quarter and mean temperature of the driest quarter. By 2070, *I. scapularis* was expected to retract by as much as 60% from southern and central regions of the state as compared to historical climate distribution but remained concentrated in the Chicago metropolitan area. *A. americanum* was predicted to initially expand across parts of east- and west-central Illinois by 2050, but then largely retract in distribution to along rivers and water bodies by 2070. The ranges of *D. variabilis* and *A. maculatum*, however, were predicted to contract in the 2050 climate scenario, but then expand in the 2070 scenario. Predicting where ticks may invade and concentrate as the climate changes will be important to anticipate, prevent, and treat TBD in Illinois.

Simple Summary: The variable landscape of Illinois creates a patchwork of tickborne disease risk to humans and domestic animals that can be predicted in part based on climate and landscape features. We fit individual and mean-weighted ensemble species distribution models for *Ixodes scapularis*, *Amblyomma americanum*, *Dermacentor variabilis,* and a newly invading tick species, *Amblyomma maculatum* using a variety of landscape and mean climate variables and identify numerous environmental niche factors that are associated with presence of these vectors in current and future climate scenarios within the state. As the environment changes over the coming decades, the distribution of these tick species will change as they adapt to the increasing temperatures and precipitation alterations. Knowing where ticks may concentrate will be important to anticipating, preventing, and treating tickborne disease.

Keywords: Ticks; species distribution models; habitat suitability models; Illinois; climate

1. Introduction

 doi:10.20944/preprints202211.0490.v1

Ticks and their associated pathogens present a growing public and veterinary health threat in the United States. Human-induced climate and landscape alterations are driving increased prevalence of emerging tick-borne diseases (TBDs) (Diuk-Wasser et al. 2021) including bacterial, rickettsial, protozoal, and viral organisms (Savage et al. 2017; Paddock and Goddard et al. 2015). These pathogen emergences are increasingly relevant as the ranges (Raghavan et al. 2021; Molaei et al. 2022) and activity periods (Raghavan et al. 2021) of native and invasive tick species (Paddock and Goddard 2015; Rochlin et al. 2019) shift, putting these vectors into greater contact with humans, companion animals, and livestock. Economically, changes in tick and TBD ecology are triggering millions of dollars in healthcare and livestock impacts (Hook et al. 2022).

Ticks are highly sensitive to and constrained by weather and climate variables (Ogden et al. 2014; Bacon et al. 2021), as well as landscape features like vegetation and land-use patterns that impact habitat fragmentation (Allan et al. 2003; Brownstein et al. 2005; Diuk-Wasser et al. 2021). In general, the questing and phenological activity, development, and survival of common tick species of medical concern are directly correlated with higher levels of humidity and warmer temperatures (Berger et al. 2014a; b; Ogden et al. 2014; Ostfeld & Brunner 2015). However, these impacts are species-specific. Ticks like *Ixodes scapularis* are highly susceptible to desiccation, whereas *Amblyomma americanum, Amblyomma maculatum,* and *Dermacentor variabilis* are more tolerant of drier conditions (Bacon et al. 2021; Rynkiewicz & Clay 2014). Greater tick density is often associated with habitats that include uninterrupted forest cover (Heske 1995; Ferrell & Brinkerhoff 2018), or even specific invasive types of landscape cover (Noden & Dubie 2017), but edge-effects and open-landscape can also foster high tick abundance depending on species (Rynkiewicz & Clay 2014; Flenniken et al. 2022). These landcover and climate relationships are critical to the landscape epidemiology of TBD because they generate the microclimatic conditions that facilitate interactions among ticks and their hosts (Randolph & Storey 1999; Diuk-Wasser et al. 2021).

The greater U.S. Midwest is on the leading edge of tick and TBD expansion. Within the past decade, studies have documented the continued range movement of four ticks of medical and veterinary concern in this region including the blacklegged tick (*Ixodes scapularis*) (Rydzewski et al. 2011; Lockwood et al. 2018), lone star tick (*Amblyomma americanum*) (Springer et al. 2014; Fowler et al. 2022), American dog tick (*Dermacentor variabilis*) (Boorgula et al. 2020; Martin et al. 2022), and Gulf Coast tick (*Amblyomma maculatum*) (Lockwood et al. 2018; Phillips et al. 2020; Alkishe & Petersen 2022; Flenniken et al. 2022). These range expansions have corresponded with an increase in reported TBD cases associated with these species including Lyme disease (Robinson et al. 2015), ehrlichiosis (Johnson et al. 2015), tidewater fever (Phillips et al. 2020) and newly documented Heartland virus (Tuten et al. 2020).

Illinois is experiencing tick and TBD expansion in both the northern and the southern regions (Springer et al. 2014; Sonenshine et al. 2018; Gilliam et al. 2020; Kopsco et al. 2021). Concurrently, there has been a 10-fold increase in commonly reported TBD cases among humans between 1999 and 2017 (IDPH 2017a, b; IDPH 2018; Lyons et al. 2021), including Lyme disease, Rocky Mountain spotted fever, ehrlichiosis, and

 doi:10.20944/preprints202211.0490.v1

anaplasmosis. Three distinct climate regions exist longitudinally across the state, with clear impacts on tick species abundance (Bacon et al. 2021). As climate alterations impact the various bioclimatic factors across these areas, it is important to predict how tick distribution and TBD risk will potentially change across the state.

While there is debate about the specific impacts of extreme climate conditions on ticks and TBDs in the future (Ogden et al. 2020), climate projection models can predict and assess various current and future habitat and distribution scenarios. Species distribution models (SDM) represent a suite of statistical and machine-learning methods for predicting suitable species habitat ranges and niches based on known occurrence records and various environmental variables. These strategies range from deterministic (e.g. logistic regression) to stochastic (e.g. Bayesian regression trees) approaches, and utilize various levels of model validation techniques. Given differences in model performance, using SDM model ensembles may provide a more complete picture of the possibilities for tick species range variation, and opportunities for public health and veterinary partners to enact control and prevention measures where most needed (Lippi et al. 2021b; Kopsco et al. 2022).

The objective of this study was to fit and evaluate current and future species distribution models for each of the four tick species of major medical and veterinary concern within Illinois, including *Ixodes scapularis*, *Dermacentor variabilis*, *Amblyomma americanum*, and *Amblyomma maculatum*, and to evaluate habitat and climate variables associated with their predicted occurrence. We expected that as the climate continues to warm, regions in southern and central Illinois will become less hospitable for a desiccant-sensitive species like *Ixodes scapularis*, but more habitable for the other three more desiccant-tolerant species. This hypothesis would reflect a greater predicted species range throughout the state for *Dermacentor* and *Amblyomma* species but would result in a growing absence of suitable *Ixodes scapularis* habitat, except in the northernmost part of the state.

 doi:10.20944/preprints202211.0490.v1

2. Materials and Methods

Tick Occurrence Data

We sourced presence-only tick occurrence records from several online, publicly accessible databases and through active tick collections throughout Illinois. Databases included Walter Reed Biosystematics Unit's VectorMap (http://vectormap.si.edu/), Global Biodiversity Information Facility (GBIF; https://www.gbif.org/), Biodiversity Information Serving Our Nation (BISON; https://bison.usgs.gov/). To be included in a model, all tick occurrence data had to meet the following quality control criteria: be an observation from no earlier than 1950, include two decimal places or more for at least one coordinate, and have a coordinate inaccuracy of ≤20,000 m. Duplicate coordinates occurred often due to data being deposited in multiple databases, so entries were compared and duplicate coordinates were removed. Geolocations were cross-checked to ensure that records were accurate to the field location. Remaining coordinates were then thinned to 1km distance using the spThin package (Aiello-Lammens et al. 2015) to reduce the effect of sampling bias on model predictions.

Environmental covariates

Bioclimatic variables (1-19) (**Table 1**) were sourced from the *raster* package (Hijmans 2022) and downloaded at a resolution of 2.5 arcminutes (~4km). Current climate models were fit using the historical data representing the average measurements from 1970-2000. Future climate models were fit with mean projections of these data at a 4km resolution using Coupled Model Intercomparison Project phase 5 (CMIP5)/ACCESS 1-0 Representative Concentration Pathway (RCP) 8.5 for 2050 (average from 2041-2060) and 2070 (average from 2061- 2080). CMIP5's ACCESS 1.0 model incorporates long-term simulation data of the 20th century climate including solar, volcanic, stratospheric aerosol, anthropogenic aerosol, emissions, and greenhouse gas concentrations (Lewis 2013). RCP 8.5 is a future climate scenario that describes the expected baseline high greenhouse gas impact resulting from a lack of carbon emission mitigation policies (Riahi et al. 2011).

Due to the importance of white-tailed deer (*Odocoileus virginianus*) as reproductive hosts for each of these four species, we included a raster of graded suitable deer habitat within Illinois (USGS 2018). Landcover covariates (landcover class, percent impervious surface, and percent tree canopy cover) from the National Land Cover Database (NLCD) (Yang et al. 2018) were also included. The NLCD is a collection of land cover imagery at 30m resolution that combines information from all years of land cover change (2001-2016) across 16 classes of cover that include impervious land, cropland, wetland, and various vegetation types, which were aggregated into seven more general land cover categories (Water, Developed, Barren, Forest, Grass/Shrub, Cropland, and Wetland). Land cover changed significantly across the United States between 2001-2016, so an average of these land covers taken from every 2-3 years was used instead of data from a single year. Elevation was sourced from the *raster* package (Hijmans 2022) derived from Shuttle Radar Topography Mission (SRTM) National Elevation Dataset digital elevation models (at a resolution of 1 and 1/3 arcseconds; USGS 2022).

 doi:10.20944/preprints202211.0490.v1

All covariates were cropped to the extent of the Illinois' state borders (xmin: -91.5, xmax: -87.5, ymin: 36.9, ymax: 42.5) and resampled to a resolution of four kilometers (2.5 arcseconds) to match the bioclimatic data set. Extracted covariate values were assessed for collinearity for each species and period by assessing variance inflation factor. Any variable with a v-step score of 10 or higher was excluded from that model due to collinearity.

Model fitting and evaluation

Models were fit using the *sdm* package (Naimi & Araujo 2016) in R version 4.1.3. Regression and machine learning models for each species for the current climate were first fit using the following individual methods: generalized linear models (GLM), generalized additive models (GAM), Bayesian regression trees (BRT), classification and regression trees (CART), MaxEnt, random forest (RF), multivariate adaptive regression splines (MARS), and support vector machines (SVM). The number of randomly selected background points were set at approximately the same number of presence points for each species due to the mixed use of regression and machine learning techniques within the modeling algorithm (Barbet-Massin et al. 2012). Cross-validation and bootstrap data partitioning methods (with 30% test percentage) were used for each model type, with five replicates for each method totaling five replicates per algorithm (30 total replicates per species). Single model algorithms that were not 100% successful during replicate runs were excluded from ensemble models. Models were evaluated using several performance scores including threshold-dependent and threshold-independent methods: area under the curve (AUC), true skill statistic (TSS), model deviance, and prevalence. Single models demonstrating AUC > 0.75, and TSS > 0.40 were retained for mean-weighted ensemble models (i.e. a two-step process that incorporates both within-model averaging and between-model averaging). Cohen's kappa was not used for single model evaluation due to its overreliance on prevalence but was consulted to determine consistency in predictions across models (Grimmett et al. 2020). AUC was not used alone to assess prediction accuracy because of its poor ability to reliably assess presence-background nature of the tick occurrence data (Allouche et al. 2006; Grimmett et al. 2020).

Preprints (www.preprints.org) | NOT PEER-REVIEWED | Posted: 28 November 2022 doi:10.20944/preprints202211.0490.v1

Table 1. Descriptions and sources of each of the 19 bioclimatic variables (WorldClim) and other environmental predictor variables (n=30) used in model fitting.

VARIABLE	DESCRIPTION	UNIT	SOURCE*
BIO1	Annual Mean Temperature	°C*100	WorldClim
BIO2	Mean Diurnal Range (Mean of monthly (max temp - min temp))	°C*100	WorldClim
BIO3	Isothermality (BIO2/BIO7) (×100)	%	WorldClim
BIO4	Temperature Seasonality (standard deviation ×100)	° C	WorldClim
BIO5	Max Temperature of Warmest Month	°C*100	WorldClim
BIO6	Min Temperature of Coldest Month	°C*100	WorldClim
BIO7	Temperature Annual Range (BIO5-BIO6)	°C*100	WorldClim
BIO8	Mean Temperature of Wettest Quarter	°C*100	WorldClim
BIO9	Mean Temperature of Driest Quarter	°C*100	WorldClim
BIO10	Mean Temperature of Warmest Quarter	°C*100	WorldClim
BIO11	Mean Temperature of Coldest Quarter	°C*100	WorldClim
BIO12	Annual Precipitation	mm	WorldClim
BIO13	Precipitation of Wettest Month	mm	WorldClim
BIO14	Precipitation of Driest Month	mm	WorldClim
BIO15	Precipitation Seasonality (Coefficient of Variation)	mm	WorldClim
BIO16	Precipitation of Wettest Quarter	mm	WorldClim
BIO17	Precipitation of Driest Quarter	mm	WorldClim
BIO18	Precipitation of Warmest Quarter	mm	WorldClim
BIO19	Precipitation of Coldest Quarter	mm	WorldClim
ELEVATION	Height above sea level	m	USGS SRTM
DEER HABITAT	Suitable white-tailed deer habitat	esence/absence	USGS GAP Analysis
LANDCOVER TYPE	Water bodies, tree canopy, developed, impervious, barren, forest, grassland, cropland, wetland	%	NLCD

*WorldClim [http://www.worldclim.com], USGS SRTM [https://www.usgs.gov/centers/eros/science], USGS Gap Analysis [https://gapanalysis.usgs.gov/apps/species-data-download/], NLCD [https://www.mrlc.gov/data/nlcd-2019-land-cover-conus]

3. Results

3.1. *Ixodes scapularis* models

After duplicate records were removed and presence points thinned there remained 62 known *I. scapularis* occurrence points across Illinois, and 70 background points randomly generated. After assessing for multicollinearity amongst environmental variables for the historical climate, seventeen predictor variables out of the 30 total environmental covariates were removed from the dataset due to v-step scores greater than 10 (bio1, bio2, bio4, bio5, bio6, bio11, bio12, bio14, bio15, bio16, bio17, bio18, bio19, percent

 doi:10.20944/preprints202211.0490.v1

developed land, percent forest canopy cover, percent white-tailed deer habitat, and percent impervious cover). Retained in the historical climate correlate dataset for *I. scapularis* were bio3, bio7, bio8, bio9, bio10, bio13, elevation, percent water body coverage, percent barren land, percent forest, percent grassland, percent cropland, and percent wetland. Future climate scenarios exhibited different collinearity patterns. Sixteen highly multicollinear variables (i.e. 2050: bio1, bio2, bio5, bio6, bio7, bio10, bio11, bio12, bio13, bio14, bio16, bio17, percent developed land, percent white-tailed deer habitat, percent canopy cover, and percent impervious cover) were removed from both the 2050 and 2070 environmental variable set, and retained were: bio3, bio4, bio8, bio9, bio15, bio18, elevation, and percent water body cover, percent barren land, percent forest cover, percent cropland, percent grassland, and percent wetland.

Single algorithm evaluation revealed RF to be the best fit model for predicting the historical climate distribution of *I. scapularis* (**Table 2**). The landscape variables that most strongly predicted occurrence of *I. scapularis* habitat across this model in the historical climate were percentage cropland (16.6% relative contribution), percent wetland (15.1%), and percent water body (11.1%). Climate variables all contributed less than 5% each. Increasing presence of *I. scapularis* was predicted on landscapes that were more than at least 1% barren land, while increasing percentages of other landscape types had negative correlations with occurrence of *I. scapularis*, namely percent cover of cropland and wetland (**Fig. 1a**). *I. scapularis* predicted occurrence rose but then dropped steeply from over 88% to below 80% as mean temperatures rose in the warmest quarter (bio10) and as annual temperature ranges (bio7) increased (**Fig. 1b**). However, increasing amounts of precipitation in the wettest months (bio16) and increasing mean temperature in the wettest quarter (bio8) were associated with a greater chance of *I. scapularis* occurrence in the historical climate period (**Fig. 1b**).

The best fit single algorithm model for future predictions (both 2050 and 2070) was RF (AUC = 0.82, correlation=0.55, TSS = 0.64, deviance = 1.08). Important environmental variables changed in contribution to the likelihood of *I. scapularis* presence in these scenarios. Landcover categories percent water bodies (19.9% relative contribution), percent wetland (17.2%) and percent cropland (14.6%) were the three most important variables contributing to the landcover predictors for future *I. scapularis* distribution in 2050 (**S1a**). Expected presence of *I. scapularis* dropped from 70% to below 60% as percent cropland rose above 50%. Both percent water bodies and wetland were associated with high expected occurrence of *I. scapularis.* Precipitation of the warmest quarter (mm; bio18) and temperature seasonality ((standard deviation ×100); bio4) were the two most important variables contributing to climate predictors of *I. scapularis* 2050 future distribution (**S1b**). As day-to-night temperature oscillations (bio3) increased by a difference of 30%, and as the overall variation (i.e. standard deviation) in the annual temperature (bio4) rose above 1000 the likelihood of *I. scapularis* presence was reduced below 80%. Notably, expected presence of *I. scapularis* dropped precipitously for both the mean temperature of the wettest (bio8) and driest (bio9) quarters as temperatures rose (**S1b**). Precipitation of the warmest quarter needed to be at least 210mm for *I. scapularis* occurrence to be expected at approximately 80% likelihood.

 doi:10.20944/preprints202211.0490.v1

In the 2070 climate scenario, percent cropland rose to nearly 30% relative contribution to the model (29.4%), followed by percent wetland (13.6%), elevation (13.2%) and percent water bodies (11.7%). No single climate variable was more contributory than another in this scenario. Increased percentage of cropland continued to be negatively associated with the presence of *I. scapularis*, dropping from just under 50% likelihood of occurrence to approximately 30%. Elevation above 175m increased the likelihood of occurrence to just under 40%. Percent water body and wetland land cover above 10% were important in predicting stable occurrence of *I. scapularis.* The highest predicted likelihood of *I. scapularis* was approximately 40% for climate predictors in the 2070 scenario, with increasing seasonal variation in precipitation (bio15) and temperature (bio4) having the largest negative impact on expected *I. scapularis* presence.

Best fit mean-weighted ensemble models for both historical and future climate scenarios included the following algorithms: GLM, BRT, MaxEnt, RF, MARS, and SVM. Within the historical climate the best fit ensemble models predicted that *I. scapularis* would most likely be found within the Chicago metropolitan region along the northeastern border of Lake Michigan, along riparian zones in western and central Illinois, and within the forested region of east-central and southern Illinois (**Fig. 2a**). The tick was also expected to be found scattered throughout pockets within the central portion of the state. As the climate warmed in the 2050 (**Fig. 2b**) and 2070 (**Fig. 2c**) projection scenarios, the likelihood of *I. scapularis* presence throughout the central and southern tiers began to recede and concentrate along rivers and waterbodies (2050), and then shifted to a greater expectation of occurrence only in the Chicago metropolitan area and along select portions of the Illinois and Sangamon Rivers (2070) (**Fig. 3**).

Preprints (www.preprints.org) | NOT PEER-REVIEWED | Posted: 28 November 2022 doi:10.20944/preprints202211.0490.v1

Table 2. Mean best fit single model evaluation metrics for the predicted historic occurrence in Illinois of the four tick species modeled. Bolded numbers denote the AUC/correlation/true skill statistic (TSS) score/deviance for the best fit model. Best fit *Amblyomma maculatum* models included CART instead of BRT.

	Species	*Ixodes scapularis*	*Amblyomma americanum*	*Dermacentor variabilis*	*Amblyomma maculatum*	*Ixodes scapularis*	*Amblyomma americanum*	*Dermacentor variabilis*	*Amblyomma maculatum*	*Ixodes scapularis*	*Amblyomma americanum*	*Dermacentor variabilis*	*Amblyomma maculatum*	*Ixodes scapularis*	*Amblyomma americanum*	*Dermacentor variabilis*	*Amblyomma maculatum*
	Number of occurrence points used	62	99	290	15	62	99	290	15	62	99	290	15	62	99	290	15
	Evaluation Metric	**AUC**				**Correlation**				**TSS**				**Deviance**			
Algorithm*	*GLM*	0.68	0.74	0.80	0.64	0.32	0.41	0.52	0.29	0.43	0.46	0.53	0.44	1.38	1.31	1.12	11.0
	BRT/CART	0.74	0.76	0.80	0.49	0.40	0.45	0.52	0.02	0.49	0.48	0.54	0.12	1.14	1.20	1.16	3.64
	MaxEnt	0.69	0.75	0.81	0.74	0.31	0.43	0.53	0.42	0.45	0.47	0.55	0.61	1.39	1.20	1.11	1.32
	RF	**0.82**	**0.76**	0.80	0.60	**0.55**	**0.44**	0.54	0.17	**0.64**	**0.49**	0.55	0.46	**1.08**	**1.20**	1.08	1.34
	MARS	0.67	0.67	0.79	0.67	0.31	0.30	0.52	0.33	0.40	0.38	0.52	0.42	6.01	2.43	1.22	21.2
	SVM	0.79	0.76	**0.81**	**0.75**	0.47	0.43	**0.55**	**0.53**	0.59	0.47	**0.55**	**0.63**	1.09	1.20	**1.07**	**1.26**

*GLM = Generalized linear models; BRT = Bayesian regression trees; CART = classification and regression tree; MaxEnt = Maximum entropy; RF = random forest; MARS = multivariate adaptive regression splines; SVM = support vector machines

Preprints (www.preprints.org) | NOT PEER-REVIEWED | Posted: 28 November 2022 doi:10.20944/preprints202211.0490.v1

Table 3. Relative percent contribution of habitat suitability variables in best fit models for each tick species across the three climate scenarios. Current climate models were fit using the historical data representing the average climate measurements from 1970-2000. Future climate models were fit with mean projections of these data at a 4km resolution using Coupled Model Intercomparison Project phase 5 (CMIP5)/ACCESS 1-0 Representative Concentration Pathway (RCP) 8.5 for 2050 (average from 2041-2060) and 2070 (average from 2061- 2080). All landscape variables represent percentage of that landcover, except for elevation which is measured in meters. The top three most important variables in the model prediction are bolded for each period. Variables that were not included in a model due to collinearity are denoted with a dash.

Environmental Variable*	Tick Species											
	Ixodes scapularis			*Amblyomma americanum*			*Dermacentor variabilis*			*Amblyomma maculatum*		
	Climate Scenario											
	Hist.	2050	2070	Hist.	2050	2070	Hist.	2050	2070	Hist.	2050	2070
Barren	0.7	1.3	2.0	1.7	1.1	1.0	2.6	2.7	1.7	7.6	-	1.3
Canopy	**-**	**-**	**-**	-	-	-	-	**-**	-	**13.7**	9.3	2.7
Cropland	**16.6**	**13.0**	**29.4**	-	-	-	**60.3**	**68.9**	**44.4**	**38.1**	**34.0**	-
Developed	-	-	-	2.7	1.9	1.3	-	-	-	-	-	**19.2**
Elevation	2.6	2.8	**13.2**	2.4	1.7	**4.8**	3.7	3.0	5.6	10.9	9.1	6.8
Forest	1.4	0.5	-	**6.2**	**5.5**	4.6	3.8	10.9	4.0	-	-	-
Grassland	0.5	0.2	-	2.0	0.7	1.4	4.7	5.1	0.9	**25.3**	13.6	**14.6**
Water	**11.1**	**20.4**	**11.7**	3.6	**13.0**	**4.7**	2.9	5.2	2.9	-	12.3	2.1
Wetland	**15.1**	**13.7**	**13.6**	2.7	1.7	3.7	5.0	1.9	4.3	4.7	6.4	2.4
BIO2	-	-	-	0.7	-	0.7	3.4	-	-	-	-	-
BIO3	0.1	0.0	0.0	-	0.2	-	-	2.3	9.1	-	-	-
BIO4	-	0.9	1.0	-	-	**12.9**	-	4.7	6.8	-	-	-
BIO6	-	-	-	-	-	-	-	-	33.8	-	-	-
BIO7	1.5	-	-	-	**4.8**	-	**17.2**	-	-	-	-	-
BIO8	0.8	1.0	0.6	1.5	0.8	-	3.6	**20.5**	**25.3**	-	-	-
BIO9	0.5	0.8	0.0	**5.0**	0.8	-	2.3	10.4	**22.6**	-	-	-
BIO10	1.6	-	-	1.9	1.4	-	1.8	-	-	-	-	-
BIO13	0.8	-	-	-	-	-	-	-	-	-	-	-
BIO15	-	0.0	0.6	**4.1**	0.3	0.3	-	3.2	8.4	10.8	-	**12.0**
BIO16	-	-	-	-	-	-	-	-	-	-	**45.8**	-
BIO17	-	-	-	-	3.7	2.2	-	-	-	-	**13.9**	-
BIO18	-	0.2	0.2	1.5	3.6	0.7	**7.8**	**13.2**	15.5	7.1	-	-
BIO19	-	-	-	-	-	-	-	-	-	-	-	1.9

* BIO1, BIO5, BIO11, BIO12, BIO14, and white-tailed deer habitat were not included due to multicollinearity. BIO2 = Mean Diurnal Range (Mean of monthly (max temp - min temp)), BIO3 = Isothermality (BIO2/BIO7) (×100), BIO4 = Temperature Seasonality (standard deviation ×100), BIO6 = Minimum Temperature of Coldest Month, BIO7 = Temperature Annual Range (BIO5-BIO6), BIO8 = Mean Temperature of Wettest Quarter, BIO9 = Mean Temperature of Driest Quarter, BIO10 = Mean Temperature of Warmest Quarter, BIO13 = Precipitation of Wettest Month, BIO15=Precipitation Seasonality (Coefficient of Variation) , BIO16 = Precipitation of Wettest Quarter, BIO17 = Precipitation of Driest Quarter, BIO18 = Precipitation of Warmest Quarter, BIO19 = Precipitation of Coldest Quarter

Preprints (www.preprints.org) | NOT PEER-REVIEWED | Posted: 28 November 2022 doi:10.20944/preprints202211.0490.v1

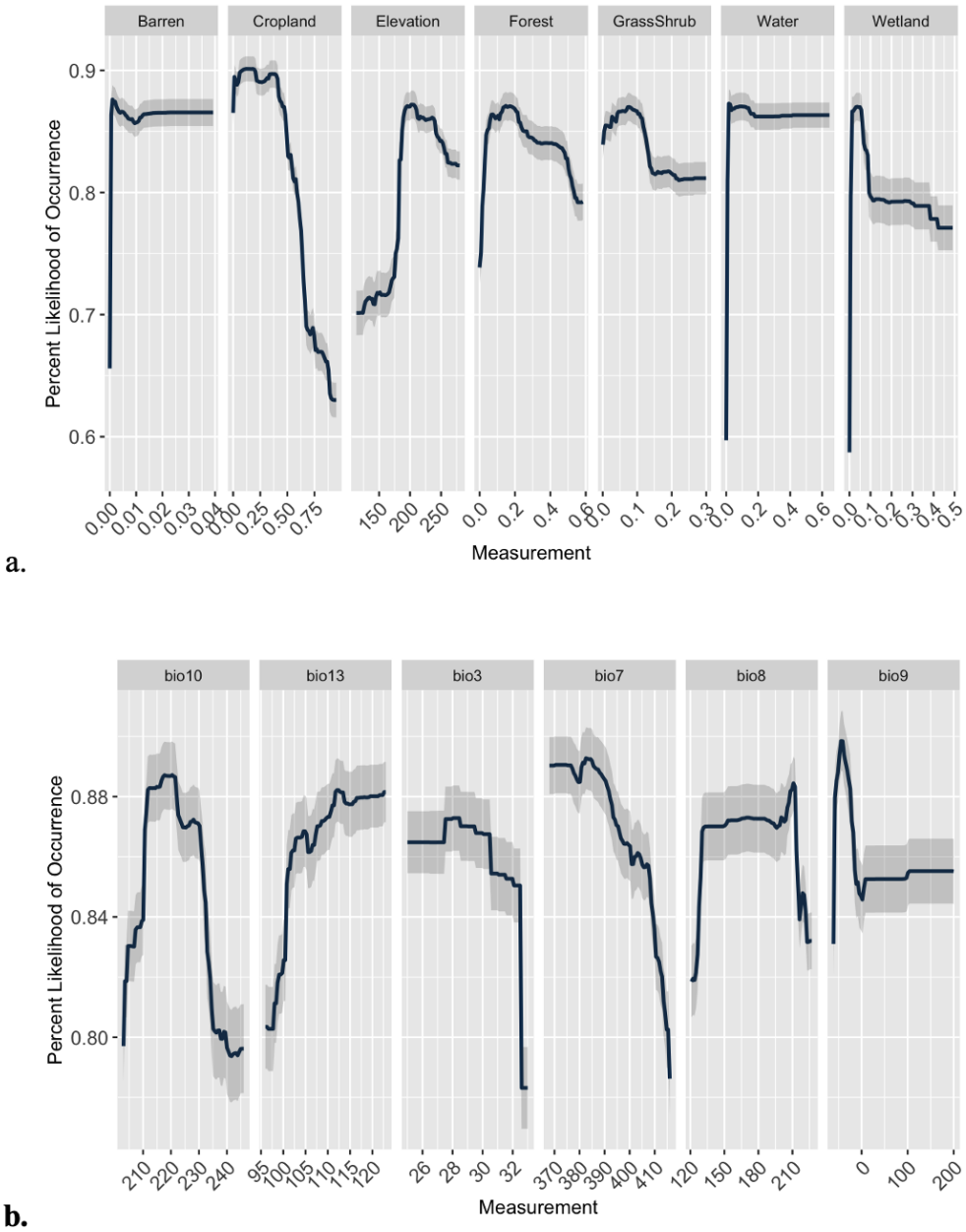

Fig. 1. Mean a) landscape feature and b) climate variable response curves for predicted probabilities of *I. scapularis* habitat in the best fit model for the historical climate. Landcover types are reported in percent coverage. Elevation is reported in meters. bio10 = mean temperature of warmest quarter (°C*100); bio13 = precipitation of the wettest month (mm); bio3 = day-to-night temperature oscillation relative to summer-winter (annual) oscillations (bio2/bio7) (x100); bio7 = temperature annual range (bio5-bio6); bio8= mean temperature of wettest quarter (°C*100); bio9 = mean temperature of the driest quarter (°C*100).

Preprints (www.preprints.org) | NOT PEER-REVIEWED | Posted: 28 November 2022 doi:10.20944/preprints202211.0490.v1

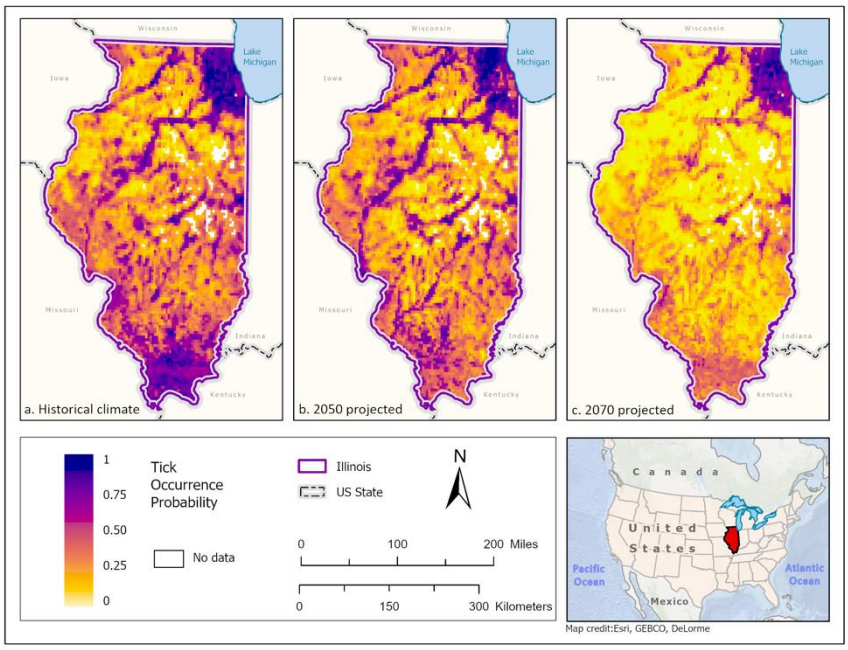

Fig. 2. a) Mean-weighted ensemble prediction of the probability of *I. scapularis* occurrence in Illinois under current historical climate conditions**. b)** Mean-weighted ensemble of predicted probability of *I. scapularis* occurrence in Illinois in 2050 projected climate Representative Concentration Pathway 8.5, ACCESS 1-0; average from 2041-2060). **c)** Mean-weighted ensemble of future predicted probability of *I. scapularis* occurrence in Illinois in 2070 projected climate (Representative Concentration Pathway 8.5, ACCESS 1-0; average from 2061- 2080). Darker colors indicate higher likelihood of tick presence.

Preprints (www.preprints.org) | NOT PEER-REVIEWED | Posted: 28 November 2022 doi:10.20944/preprints202211.0490.v1

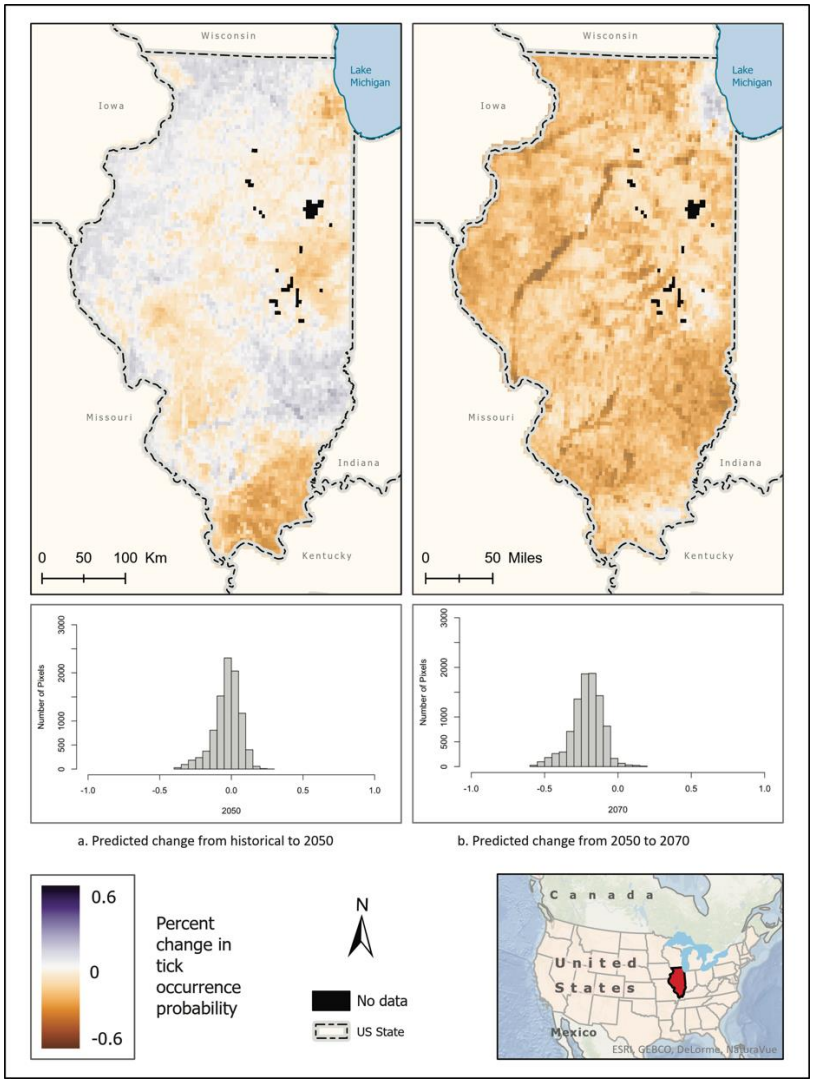

Fig. 3. Percent change in likelihood of *I. scapularis* occurrence between the historical climate and 2050 (left) and from 2050 to 2070 (right). Red shades indicate reduced likelihood of occurrence (negative change), blue shades indicate increased likelihood of occurrence (positive change). The histogram represents the number of pixels (y-axis) containing the binned percentage likelihood (x-axis) of *I. scapularis* suitable habitat across the map.

3.2 *Amblyomma americanum* models

After removing duplicate observations and occurrence points were thinned to 1km, 99 records of *Amblyomma americanum* were retained for modeling and 100 randomly selected background points were generated. Seventeen variables were removed due to multicollinearity (bio1, bio3, bio4, bio5, bio6, bio7, bio11, bio12, bio13, bio14, bio16, bio17, bio19, percent cropland, percent canopy, and percent impervious surface, and percent white-tailed deer habitat). Retained for modeling of the historical climate were bio2, bio8, bio9, bio10, bio15, bio18 and land cover categories elevation, percent water body coverage, percent developed land, percent barren land, percent forest coverage, percent grassland, and percent wetland.

Future climate scenarios exhibited different multicollinearity patterns. The projected average climate for 2050 demonstrated collinearity issues with 15 variables (bio1, bio2, bio4, bio5, bio6, bio11, bio12, bio13, bio14, bio16, bio19, percent cropland, percent tree

 doi:10.20944/preprints202211.0490.v1

canopy, and percent impervious surface, and percent white-tailed deer habitat). Retained for the 2050 modeling environmental variable set were bio3, bio7, bio8, bio9, bio10, bio15, bio17, bio18, elevation, percent water body coverage, percent developed land, percent barren land, percent forest, percent grassland, and percent wetland. In the 2070 climate scenario, sixteen variables were removed due to collinearity issues (bio1, bio3, bio5, bio6, bio7, bio10, bio11, bio12, bio13, bio14, bio16, bio19, percent cropland, percent canopy, percent impervious surface, and percent white-tailed deer habitat) and the final model used the following: bio2, bio4, bio8, bio9, bio15, bio17, bio18, elevation, percent water body landcover, percent developed land, percent barren land, percent forest, percent grassland, and percent wetland.

Random forest was also the best fit single model algorithm for this species of the six total included model algorithms (**Table 2**). The most important variables that predicted occurrence of *A. americanum* habitat across this model for the historical climate were percent forest coverage (6.2% variable contribution) and percent water bodies present in the landscape (2.4%). Climate variables bio9 (5.0%), and bio15 (4.1%) were the most important contributing climate variables to the historical climate prediction of *A. americanum* distribution. As the percentage of forest cover increased, the likelihood of A. *americanum* presence rose sharply from just over 50% likelihood of occurrence to near 75% chance of occurrence (**Fig. 4a**). The historical climate scenario also demonstrated that *A. americanum* is positively associated with grasslands, water bodies, and wetland landcovers (**Fig. 4a)**. The probability of their occurrence also increases with mean temperature in the warmest quarters and in the driest quarters (**Fig. 4b**). Like *I. scapularis*, probability of occurrence of *A. americanum* decreases sharply with increasing annual temperature difference (**Fig 4b**).

The best fit single model for future predictions of *A. americanum* distribution was RF (AUC = 0.82, correlation= 0.55, TSS = 0.56, deviance= 1.04). In the 2050 scenario, percent water body landcover became the most important relative variable (13.0%) in predicting occurrence of *A. americanum*, followed by percent forest cover (5.5%), and demonstrated an increase in probability of presence by about 20% when percentage of the landcover type reached 50% (**S3a**). *A. americanum* became increasingly dependent on precipitation in the 2050 scenario, with large increases in predicted occurrence as the amount of precipitation rose during the driest quarter (bio17; **S3b**), and during the warmest quarter (bio18; **S3b**).

Best fit mean-weighted ensemble models for both current and future climate scenarios included the following algorithms: GLM, BRT, MaxEnt, RF, MARS, and SVM. Current *A. americanum* distribution was predicted to be concentrated in the southern-most portion of the state where there is more contiguous forest habitat but also found along riparian zones along the Illinois and Mississippi River systems, and on the outskirts of Lake Michigan (**Fig. 5a**).

As the climate scenarios progress, habitat in Southern Illinois appears to be slightly less hospitable to *A. americanum* as the central and northeastern Chicago metropolitan areas increased in likelihood of occurrence (**Fig. 5b, c**). The change in habitat suitability is reflected change in habitat suitability by 2050 initially demonstrates greater change of occurrence of *A. americanum* in the west and east central regions of Illinois, as well as the

 doi:10.20944/preprints202211.0490.v1

suburbs of Chicago (**Fig. 6**). By 2070, the greatest change in habitat suitability occurs around Chicago, the riparian zones along the Illinois River, and in southeastern Illinois, where the locations appear to be more favorable for occurrence of *A. americanum* (**Fig. 6**).

Preprints (www.preprints.org) | NOT PEER-REVIEWED | Posted: 28 November 2022 doi:10.20944/preprints202211.0490.v1

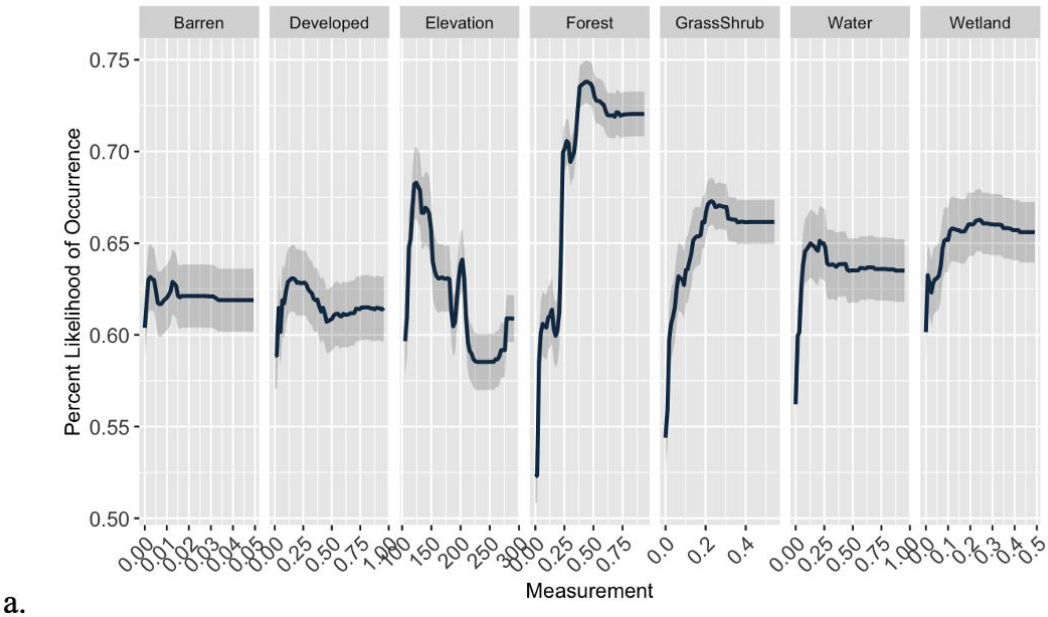

a.

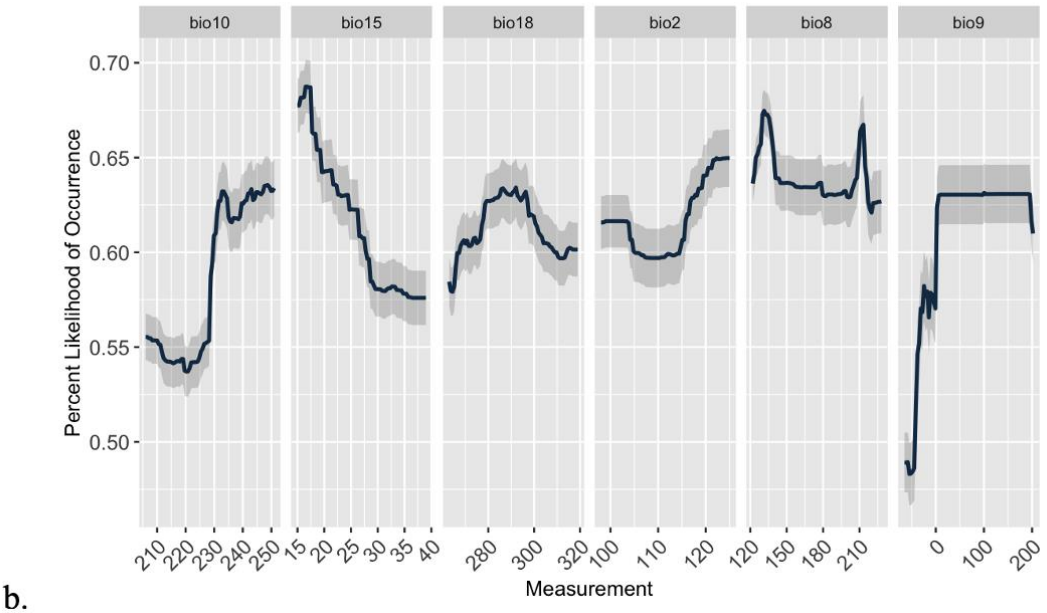

b.

Fig. 4. Mean **a)** landscape feature and **b)** climate variable response curves for predicted probabilities of *A. americanum* occurrence in the best fit model for the historical climate. Landcover classes are reported in percent coverage. Elevation is reported in meters. bio10 = mean temperature of the warmest quarter (°C*100). bio15= precipitation seasonality (mm), bio18 = precipitation in the warmest quarter (mm), bio2 = mean diurnal range (mean of monthly (max temp - min temp)) (°C*100), bio8 = mean temperature of wettest quarter (°C*100), bio9 = mean temperature of driest quarter (°C*100).

Preprints (www.preprints.org) | NOT PEER-REVIEWED | Posted: 28 November 2022 doi:10.20944/preprints202211.0490.v1

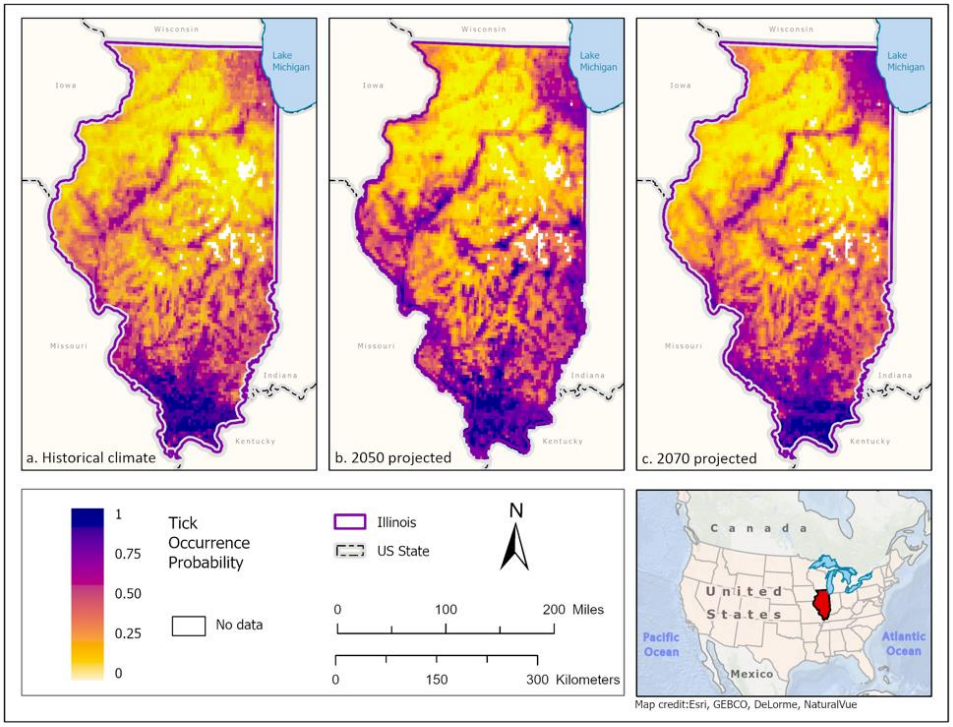

Fig. 5. a) Mean-weighted ensemble prediction of the probability of *A. americanum* occurrence in Illinois under current climate conditions. **b)** Mean-weighted ensemble of predicted probability of *A. americanum* occurrence in Illinois in 2050 projected climate Representative Concentration Pathway 8.5, ACCESS 1-0; average from 2041-2060). **c)** Mean-weighted ensemble of future predicted probability of *A. americanum* occurrence in Illinois in 2070 projected climate (Representative Concentration Pathway 8.5, ACCESS 1-0; average from 2061- 2080). Darker colors indicate higher likelihood of tick presence.

Preprints (www.preprints.org) | NOT PEER-REVIEWED | Posted: 28 November 2022 doi:10.20944/preprints202211.0490.v1

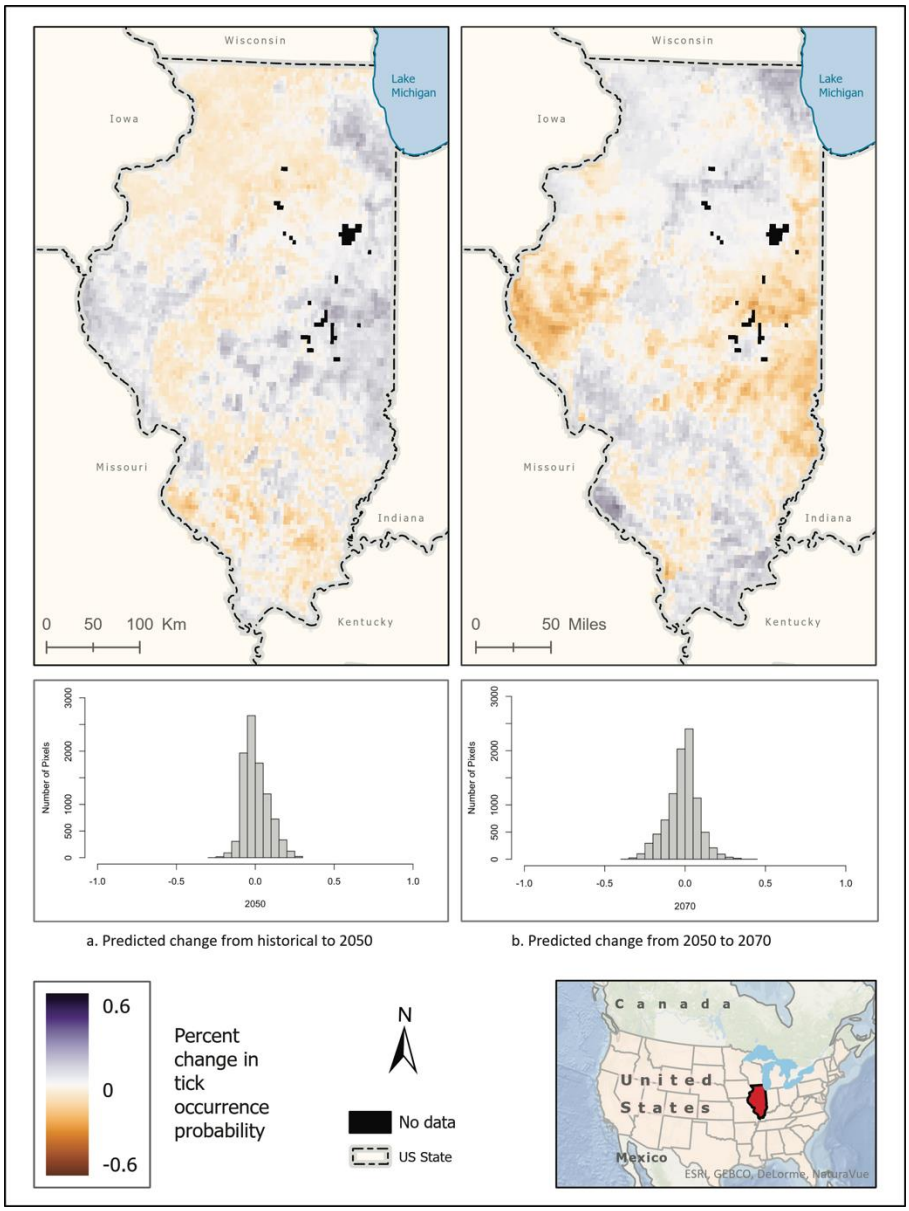

Fig. 6. Percent change in likelihood of *A. americanum* occurrence between the historical climate and 2050 (left) and from 2050 to 2070 (right). Red shades indicate reduced likelihood of occurrence (negative change), blue shades indicate increased likelihood of occurrence (positive change). The histogram represents the number of pixels (y-axis) containing the binned percentage likelihood (x-axis) of *A. americanum* suitable habitat across the map.

3.3. *Dermacentor variabilis* models

After removing duplicate records and thinning observations, 290 records of *D. variabilis* were retained for modeling and 300 randomly generated background points were generated. Best fit models for the historical climate condition for *D. variabilis* included bio2, bio7, bio8, bio9, bio10, bio18, elevation, percent water body coverage, percent barren land, percent forest, percent grassland, percent cropland, and percent wetland. Seventeen covariates (bio1, bio3, bio4, bio5, bio6, bio11, bio12, bio13, bio14, bio15, bio16, bio17, bio19, percent canopy cover, percent impervious surface, percent developed landcover, and percent white-tailed deer habitat) were removed from consideration in the historical climate model due to collinearity issues.

 doi:10.20944/preprints202211.0490.v1

Future climate scenarios included environmental variables bio3, bio4, bio8, bio9, bio15, bio18, elevation, percent water cover, percent barren land, percent forest cover, percent grassland, percent cropland, and percent wetland for the 2050 projected climate scenario, and bio3, bio4, bio6, bio8, bio9, bio15, bio18, elevation, percent water body landcover, percent barren land, percent forest cover, percent grassland, percent cropland, and percent wetland cover for the 2070 projected climate. Seventeen variables (bio1, bio2, bio5, bio6, bio7, bio10, bio11, bio12, bio13, bio14, bio16, bio17, bio19, percent canopy cover, percent developed land, percent impervious surface, and percent white-tailed deer habitat) were removed from analysis for the 2050 scenario, and 16 covariates (bio1, bio2, bio5, bio7, bio10, bio11, bio12, bio13, bio14, bio16, bio17, bio19, percent canopy cover, percent developed land, percent impervious surface, and percent white-tailed deer habitat) were excluded from the 2070 projected climate scenario models due to collinearity issues.

Support vector machines was the best fit single model algorithm for predicting the presence of *D. variabilis* within the historical climate (**Table 2**). Percent cropland was the most important variable in predicting *D. variabilis* occurrence (60.3% relative importance), followed by percent wetland (5.4%), percent grassland (4.6%), and percent forest (3.8%) (**Fig. 7a**). Climate variables that contributed most to the model were the annual temperature range (°C*100; bio7) (17.6% relative variable importance), and precipitation of the warmest quarter (mm; bio18) (8.6%) (**Fig. 7b**).

For the 2050 climate projection, RF was the best fit model (AUC =0.81, correlation =0.55, TSS =0.55, deviance =1.06). Percent cropland was again the most important variable in predicting occurrence of *D. variabilis* (68.9% relative variable importance), followed by percent forest cover (10.9%), percent water bodies (5.2%), and percent grassland (5.1%). The mean temperature of the wettest quarter (°C*100) (bio8) was the most important climate variable to predict distribution of *D. variabilis* in the 2050 scenario (20.5% relative variable importance), followed by precipitation in the warmest quarter (mm) (13.2%; bio18), and mean temperature of the driest quarter (10.4%; bio9). As the percentage of cropland increased above 25%, the expected occurrence of *D. variabilis* declined from nearly 90% to approximately 45% likelihood (**S5a**). Under the conditions expected in this period, this species was more likely to be found in areas with more water bodies (up to 40% landcover) and expected between 70 and 80% likelihood within grassland (**S5a**). Likelihood of finding this species decreased with increasing coverage of barren land and wetland (**S5a**). Expected occurrence of *D. variabilis* initially increased to nearly 90% likelihood as the mean temperature of the wettest quarter rose, but then dropped sharply to 50% once the mean temperature reached 1.25°C (**S5b**). *D. variabilis* presence also increased in likelihood with precipitation in the warmest quarter, but then began to wane after 220mm (**S5b**). In the driest quarter, *D. variabilis* occurrence was positively associated with increasing mean temperatures (**S5b**).

In the 2070 climate projection, *D. variabilis* distribution was best predicted by a RF model (AUC=0.80, correlation = 0.52, TSS = 0.53, deviance = 1.09). Percent cropland (44.4% relative importance) and elevation (5.6%) were the most impactful landscape predictors of *D. variabilis* presence in this scenario. Climate variables were far more important in determining the probability of *D. variabilis* occurrence in this scenario. Most impactful

 doi:10.20944/preprints202211.0490.v1

were the minimum temperature of the coldest month (°C*100) (bio6; 33.8%), mean temperature of the wettest quarter (°C*100) (bio8; 25.3%), mean temperature of the driest quarter (°C*100) (bio9; 22.6%), and precipitation in the warmest quarter (mm) (bio18; 15.5%). Similar response patterns are seen in the 2070 projected climate to the 2050 climate, but with overall expected occurrence of *D. variabilis*, and more dramatic response to the changing variables. Increasing percentage of cropland reduces the overall likelihood of *D. variabilis* to 40% (**S6a**). The likelihood of *D. variabilis* was positively associated with increasing mean minimum temperature in the coldest months (bio6) and precipitation in the warmest quarter (**S6b**), but negatively associated with increasing mean temperature in the wettest months (bio8), mean temperature of the driest quarter (bio9), and increasing variation in both annual temperature (bio4) and precipitation (bio15) (**S6b**).

Best fit mean-weighted ensemble models for historical and future climate scenarios included the following algorithms: GLM, BRT, MaxEnt, RF, MARS, and SVM. Occurrence for *D. variabilis* under current climate conditions was predicted to be distributed throughout the state, with concentrations of higher probability located within southern Illinois, the Chicago metropolitan region, and along riparian zones (**Fig. 8a**). All climate scenarios predict that probability of *D. variabilis* occurrence is generally resilient in most habitats except cropland, but increasingly dependent on lower temperature and higher precipitation as the climate shifts into the more extreme 2070 projections (**Fig. 8b, c**). Along the northeastern border west of Rockford east central region of the state encompassing Champaign-Urbana and Decatur are predicted to become increasingly hospitable for *D. variabilis* as the southern tier becomes less likely to host this species due to increasing temperatures in 2050 (**Fig. 9**). By 2070, favorable habitat suitability for *D. variabilis* is expected to concentrate more broadly across the northern half of the state (**Fig. 9**).

Preprints (www.preprints.org) | NOT PEER-REVIEWED | Posted: 28 November 2022 doi:10.20944/preprints202211.0490.v1

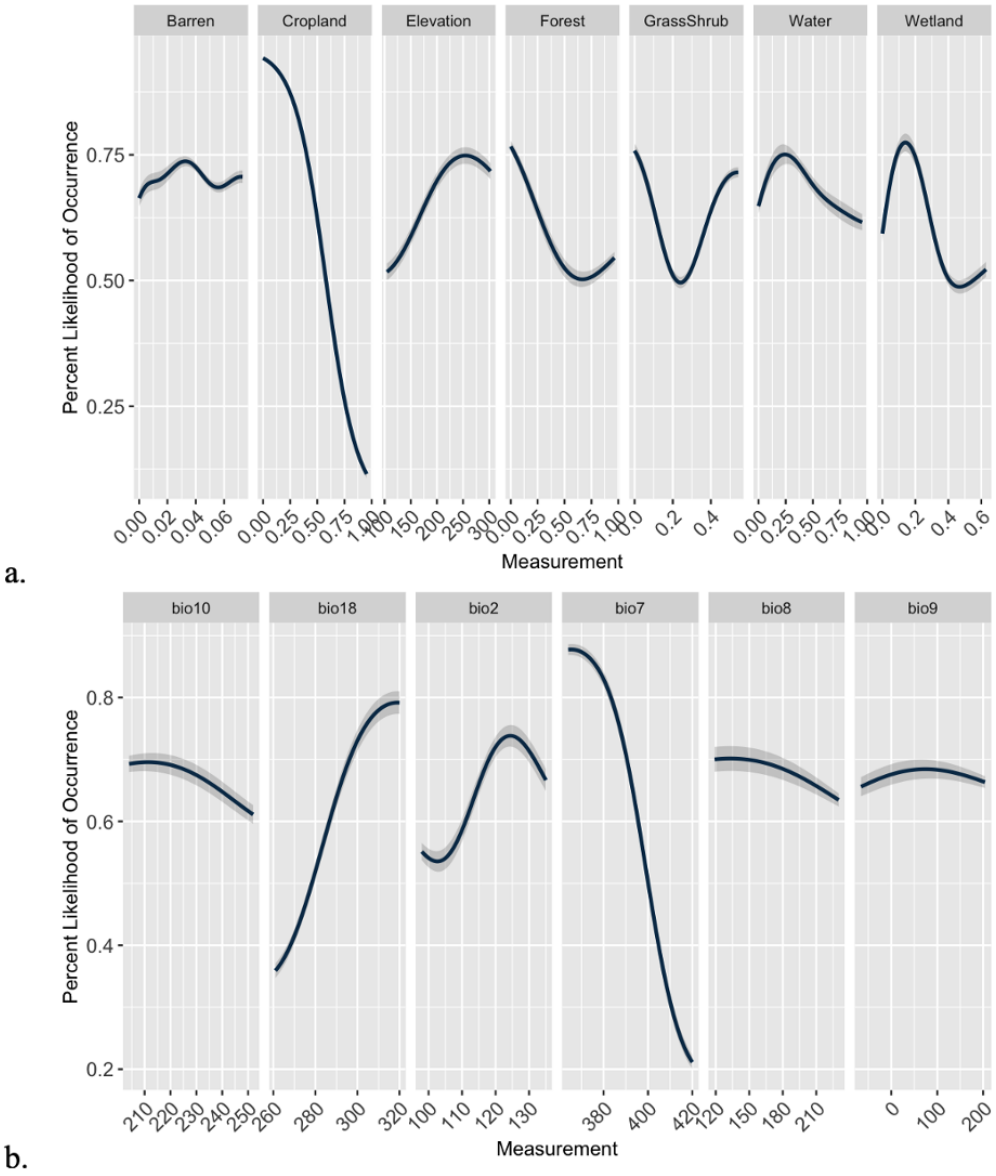

Fig. 7. Mean **a)** landscape feature and **b)** climate variable response curves for predicted probabilities of *D. variabilis* occurrence in the best fit model (random forest) for the historical climate. Landcover types are reported in percent coverage. Elevation is reported in meters. bio10 = mean temperature of the warmest quarter (°C*100), bio18 = precipitation in the warmest quarter (mm), bio2 = mean diurnal range (mean of monthly (max temp - min temp)) (°C*100), bio7 = temperature annual range (BIO5-BIO6) (°C*100), bio8 = mean temperature of wettest quarter (°C*100), bio9 = mean temperature of driest quarter (°C*100).

Preprints (www.preprints.org) | NOT PEER-REVIEWED | Posted: 28 November 2022 doi:10.20944/preprints202211.0490.v1

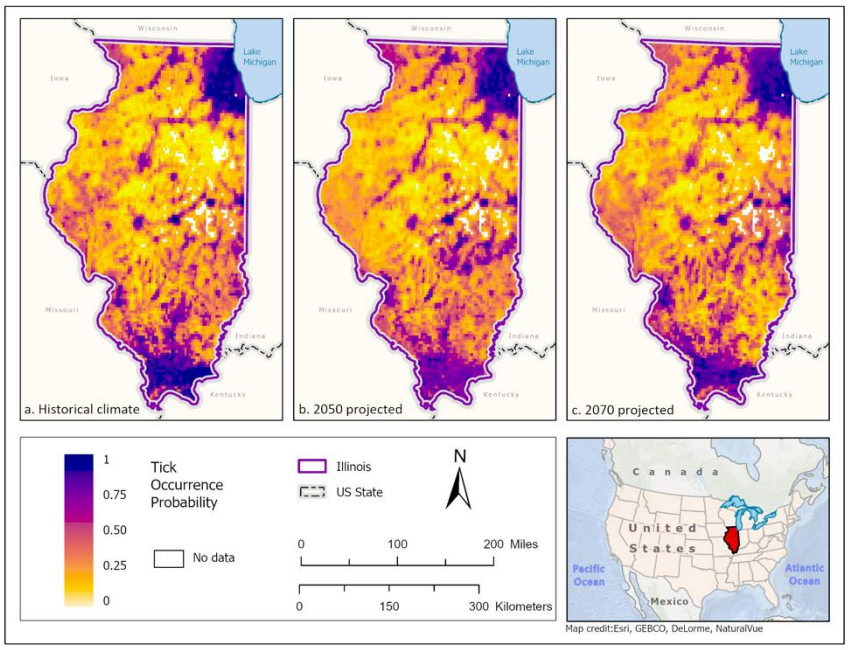

Fig. 8. a) Mean-weighted ensemble prediction of the probability of *D. variabilis* occurrence in Illinois under historical climate conditions. **b)** Mean-weighted ensemble of predicted probability of *D. variabilis* occurrence in Illinois in 2050 projected climate Representative Concentration Pathway 8.5, ACCESS 1-0; average from 2041-2060). **c)** Mean-weighted ensemble of future predicted probability of *D. variabilis* occurrence in Illinois in 2070 projected climate (Representative Concentration Pathway 8.5, ACCESS 1-0; average from 2061- 2080). Darker colors indicate higher likelihood of tick presence.

Preprints (www.preprints.org) | NOT PEER-REVIEWED | Posted: 28 November 2022 doi:10.20944/preprints202211.0490.v1

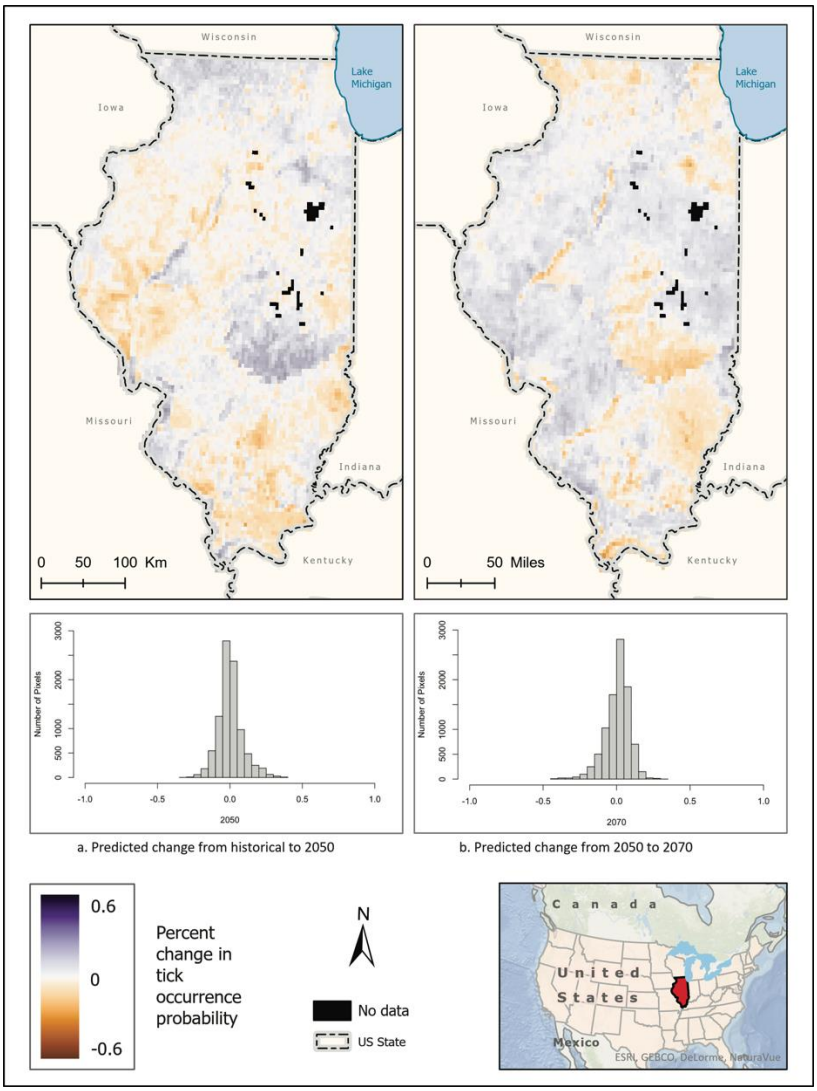

Fig. 9. Percent change in likelihood of *D. variabilis* occurrence between the historical climate and 2050 (left) and from 2050 to 2070 (right). Red shades indicate reduced likelihood of occurrence (negative change), blue shades indicate increased likelihood of occurrence (positive change). The histogram represents the number of pixels (y-axis) containing the binned percentage likelihood (x-axis) of *D. variabilis* suitable habitat across the map.

3.4. *Amblyomma maculatum* models

Fifteen records of *A. maculatum* were retained for modeling after removing duplicates and thinning, and were combined with 20 randomly selected background points. A total of twenty-one environmental correlates (bio1, bio2, bio3, bio4, bio5, bio6, bio7, bio8, bio9, bio10, bio11, bio12, bio13, bio14, bio16, bio17, bio19, percent white-tailed deer habitat, percent developed land, percent forest, and percent impervious surface) were removed due to multicollinearity. Remaining predictors in the historical climate model for *A. maculatum* were bio15, bio18, elevation, percent water body landcover, percent barren land, percent grassland, percent cropland, percent wetland, and percent tree canopy cover. The 2050 climate scenario included bio16, bio17, elevation, percent water body landcover, percent barren landscape, percent grassland, percent cropland, percent wetland, and percent canopy cover. Twenty-one variables (bio1, bio2, bio3, bio4, bio5, bio6, bio7, bio8, bio9, bio10, bio11, bio12, bio13, bio14, bio15, bio18, bio19, percent white-tailed deer habitat,

 doi:10.20944/preprints202211.0490.v1

percent developed land, percent forest, and percent impervious surface) were removed due to collinearity. The 2070 scenario included bio15, bio19, elevation, percent water body landcover, percent developed land, percent barren land, percent grassland, percent wetland, and percent canopy cover. Removed due to collinearity were bio1, bio2, bio3, bio4, bio5, bio6, bio7, bio8, bio9, bio10, bio11, bio12, bio13, bio14, bio16, bio17, bio18, percent white-tailed deer habitat, percent cropland, percent forest, and percent impervious surface.

Support vector machines was the best fit model to predict the historical distribution of *A. maculatum* (**Table 2**). Percent grassland (34.4% relative importance), percent cropland (22.4%), percent tree canopy cover (17.0%), and percent water body cover (12.2%) were the most important landscape variables in predicting probable locations of *A. maculatum*. Occurrence of this tick species was expected in open landscapes, and was positively correlated with increasing percentages of grassland, and negatively correlated with canopy cover and cropland (**Fig. 10a**). Proximity to waterbodies and wetlands also increased the probability of *A. maculatum* occurrence in the historical climate (**Fig. 10a**). Variation in precipitation as well as total precipitation in the warmest quarter initially was associated with an increase in likelihood of *A. maculatum* occurrence, but then likelihood decreased with increasing precipitation beyond a particular point (**Fig. 10b**).

Occurrence of *A. maculatum* in the 2050 climate scenario was best modelled by CART (AUC = 0.89, correlation = 0.71, TSS = 0.62, deviance = 0.69). Percent grassland, cropland, and canopy remained the most important variables for the model (18.4%, 16.3%, and 10.3% relative importance respectively). Probability of *A. maculatum* occurrence increased with increasing percentage of barren landcover and water bodies, but decreased in response to increasing percentage of cropland, elevation, grassland, and wetlands (**S7a**). Precipitation of the wettest quarter (mm; bio16) was associated with a gradual decrease in likelihood of *A. maculatum* occurrence during this time period, and precipitation of the driest quarter (mm; bio17) was associated with a small increase in probability of occurrence (**S7b**). Under the 2070 climate scenario, RF was the best fit model (AUC=0.71, correlation = 0.37, TSS = 0.61, deviance = 1.23) to describe the predicted occurrence of *A. maculatum*. In this climate, percent developed land and percent grassland were the most important landscape variables (19.9% and 14.8% relative importance respectively). Precipitation seasonality (mm; bio15) was also a driving climate variable in the prediction of *A. maculatum* distribution (12.3% relative variable importance). Within these conditions, *A. maculatum* was predicted (between 40 and 50% likelihood) to be associated with barren landscapes, but also within habitats containing roughly 20% tree canopy. Occurrence of this tick species was also expected in areas with 10-20% water bodies and wetlands. *A. maculatum* was less likely to be expected in habitats that were more than 10% grassland or above 200m elevation (**S8a**). As the variation in precipitation across seasons (bio15) increased above 27mm, the likelihood of *A. maculatum* occurrence decreased sharply from roughly 63% likelihood to below 45% probability. Increasing precipitation of the coldest quarter (bio19) was associated with a small increase in *A. maculatum* occurrence probability between 150mm and 200mm, but then decreased below 40% (**S8b**).

These model predictions suggest that *A. maculatum* has wide distribution potential throughout Illinois in the historical climate scenario. It is most likely to be able to survive

 doi:10.20944/preprints202211.0490.v1

in open barren landscapes that are close to water sources and wetlands, placing the most probable distribution predictions along the Mississippi River, Illinois River, and around the Chicago metropolitan area on the banks of Lake Michigan. Scattered pockets of higher probability throughout the state correspond with areas that are devoid of dense (greater than 50% coverage) tree canopy, or areas that are more than 50% cropland (**Fig. 11a**). In the 2050 (**Fig. 11b**) and 2070 (**Fig. 11c**) climate prediction ensemble models projected that *A. maculatum* distribution would reduce overall, with covariates only predicting likelihood of tick occurrence as high as 60%. During these scenarios, *A. maculatum* was generally more prevalent in areas with less than 50% canopy cover and up to 50% water bodies (**S7a; S8a**). In 2050, the distribution of *A. maculatum* was predicted to be more highly concentrated in the west-central part of the state, as well as near rivers and the floodplains of water bodies (**Fig. 11b**). The predictions for *A. maculatum* distribution in the 2070 scenario appear to change drastically, with higher likelihood of occurrence throughout the central portion of the state – including in areas with a high percentage of cropland – and less strongly associated with water bodies and wetlands (**Fig. 11c**). However, since cropland was removed as a variable in this model due to high collinearity, it may have skewed this prediction. Change over time shows a southwest to northeastern shift in suitable habitat across the state, with a dramatic increase of likelihood of occurrence of *A. maculatum* in the Chicago metropolitan region by 2070 (**Fig. 12**).

Preprints (www.preprints.org) | NOT PEER-REVIEWED | Posted: 28 November 2022 doi:10.20944/preprints202211.0490.v1

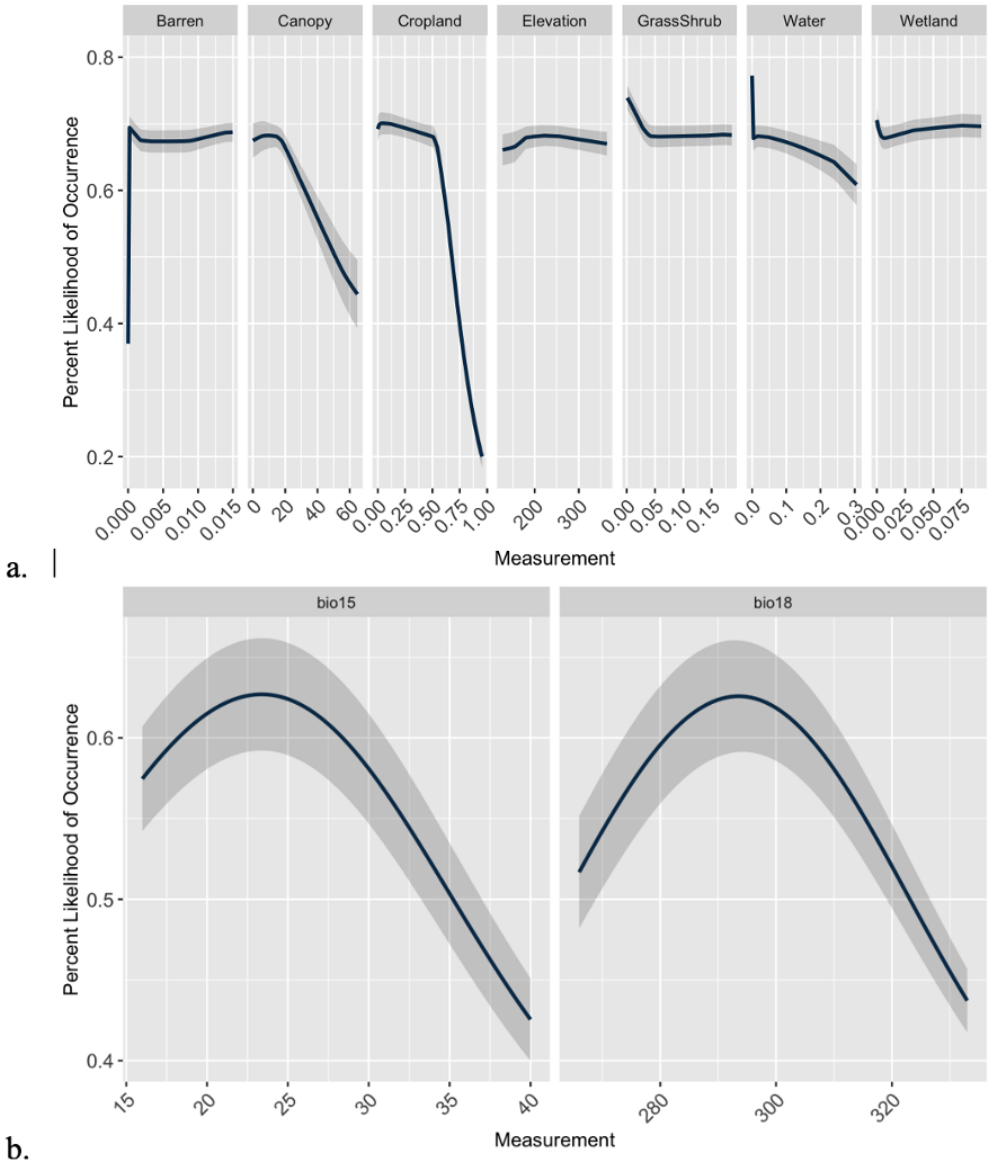

Fig. 10. Mean **a)** landscape feature and **b)** climate variable response curves for predicted probabilities of *A. maculatum* occurrence in the best fit model (MaxEnt) for the historical climate. Landcover types are reported in percent coverage. Elevation is reported in meters. bio15= precipitation seasonality (mm), bio18 = precipitation in the warmest quarter (mm).

Preprints (www.preprints.org) | NOT PEER-REVIEWED | Posted: 28 November 2022 doi:10.20944/preprints202211.0490.v1

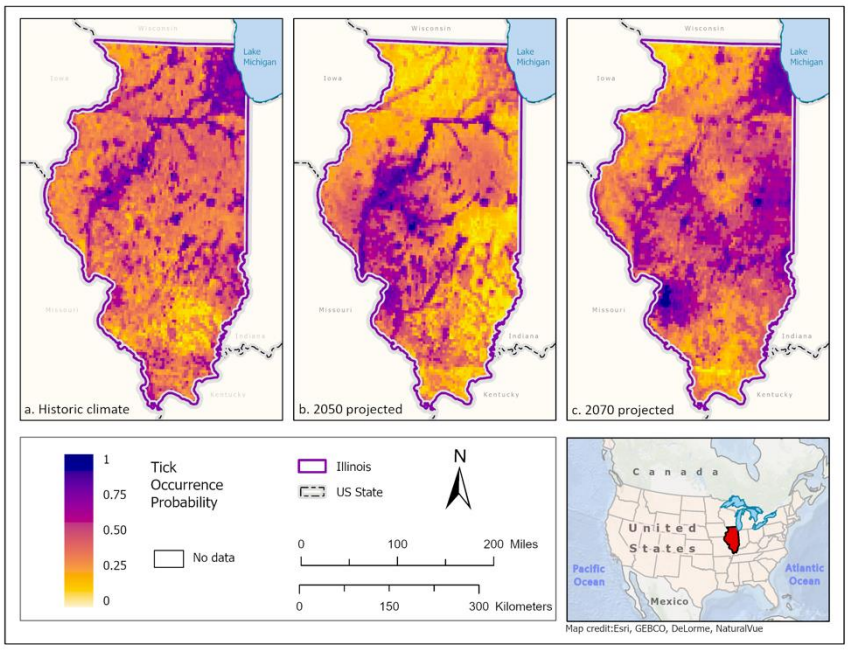

Fig. 11. a) Mean-weighted ensemble prediction of the probability of *A. maculatum* occurrence in Illinois under current climate conditions. b) Mean-weighted ensemble of predicted probability of *A. maculatum* occurrence in Illinois in 2050 projected climate Representative Concentration Pathway 8.5, ACCESS 1-0; average from 2041-2060). c) Mean-weighted ensemble of future predicted probability of *A. maculatum* occurrence in Illinois in 2070 projected climate (Representative Concentration Pathway 8.5, ACCESS 1-0; average from 2061- 2080). Darker colors indicate higher likelihood of tick presence.

Preprints (www.preprints.org) | NOT PEER-REVIEWED | Posted: 28 November 2022 doi:10.20944/preprints202211.0490.v1

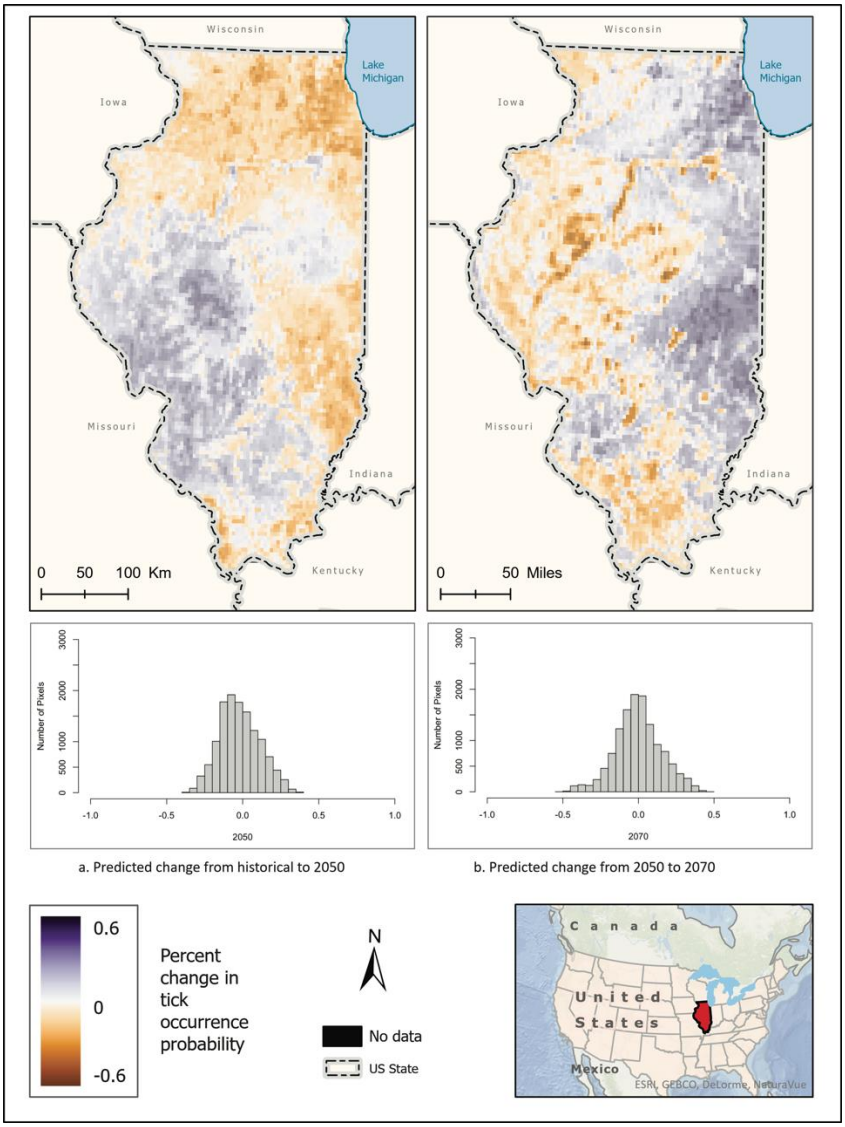

Fig. 12. Percent change in likelihood of *A. maculatum* occurrence between the historical climate and 2050 (left) and from 2050 to 2070 (right). Red shades indicate reduced likelihood of occurrence (negative change), blue shades indicate increased likelihood of occurrence (positive change). The histogram represents the number of pixels (y-axis) containing the binned percentage likelihood (x-axis) of *A. maculatum* suitable habitat across the map.

4. Discussion

This investigation applied numerous species distribution modeling techniques to examine the historically predicted distribution of four ticks of medical concern in Illinois, and the estimated future habitat suitability based on two climate scenarios. With the exception of *A. maculatum*, our results support known (Jobe et al. 2007; Rydzewki et al. 2012; Gilliam et al. 2020) and predicted (Guerra et al. 2001; Lippi et al. 2021a; Alkishe et al. 2021; Flenniken et al. 2022) habitat ranges for these species within the state and attempted to identify environmental factors that will contribute to continued or altered suitability distributions in potential future climate conditions.

 doi:10.20944/preprints202211.0490.v1

The best fit individual models to describe these historical and future habitat suitability scenarios were random forest and support vector machines. Random forest is a specific type of classification/regression tree (CART) ensemble and recursive partitioning method that can handle highly dimensional data with accuracy and is resistant to overfitting due to its randomized splitting and sampling procedure of the training data (Strobl et al. 2009). However, Valavi et al. (2021) note that RF prediction can be negatively impacted when using presence-background data like the tick data used in this investigation due to class imbalance and overlap. This occurs when there is a small sample of presence points, and the background points are sampled in a way that does not allow for enough discrimination in the predictors of presence and background location (Valavi et al. 2021). Support vector machines are another machine learning algorithm that utilize kernel function for mapping presences amidst complex correlational data and are useful because they do not require data to be independent (Drake et al. 2006; Valavi et al. 2022). To prevent biasing the outcomes as best as we could we applied mean weights, approximate equal sampling of the presence and the background data and used down-sampling by way of cross-validation (Valavi et al. 2021). The best performing models were consistently the mean-weighted ensembles, which is an outcome supported by previous research (Valavi et al. 2022).

Our models support and expand upon previous work on habitat suitability for ticks in Illinois. Records of county-level establishment, passive surveillance, and ecological niche modeling demonstrate expansion of *I. scapularis* across the state (Eisen et al. 2016; Kopsco et al. 2021; Alkishe et al. 2021; Wikel 2022), however our expectation that as the climate continues to warm, regions in southern and central Illinois will become less hospitable for a desiccant-sensitive species like *I. scapularis,* was supported. Our models predicted that *I. scapularis* will be confined to more northern regions in the state, and within habitats that provide more protective cover (e.g. upland forest) and moisture availability, e.g. along riparian zones of the Sangamon, Rock, and Illinois Rivers, as well as in forested areas and edge surrounding Lake Shelbyville, and Upper Peoria Lake. Shawnee National Forest is also expected to remain suitable through 2070, although we predicted between 0.50 and 0.75 chance of occurrence in that scenario.

We observed the potential continued future suitability of habitat for *I. scapularis* located in high population centers like Cook, DuPage, McHenry, and Lake Counties outside Chicago. *Borrelia burgdorferi*-infected *I. scapularis* have been collected from high-access areas within these locations going back decades (Jobe et al. 2007; Rydzewski et al. 2011). Guerra et al. (2002) identified positive associations of *I. scapularis* with various soil types (e.g. fertile alfisols, sand, and loam), deciduous and dry forests, and negative associations with grasslands, acidic soils, conifer, and wet forests. At that time, highly likely (>0.50) habitat suitability for *I. scapularis* was largely limited to areas within Shawnee National Forest, and along the Illinois and Mississippi River and very few areas of higher probability of presence (0.50-0.75) in the counties surrounding Chicago (Guerra et al. 2002). We predicted greater suitability for *I. scapularis* throughout the central and southern portions of the state than what was previously predicted or currently reported by Illinois Department Public Health records (IDPH 2022). It is suspected that *I. scapularis*

 doi:10.20944/preprints202211.0490.v1

is not currently occupying a larger distribution within Illinois due to its complex ecology (Kilpatrick et al. 2017; Diuk-Wasser et al. 2021; McBride et al. 2022). While our results could suggest that the tick simply has not yet invaded these areas, they may also reflect sampling limitations. Lyons et al. (2021) found few *I. scapularis* ticks during active surveillance in southern Illinois, but the timing of this surveillance was not optimized to the phenology of *I. scapularis* and passive surveillance efforts lacked coverage in many areas of interest.

Levi et al. (2015) examined activity patterns of *I. scapularis* over 19 years and found years with warmer temperatures in the summer and fall were associated with a three-week acceleration in the phenology of nymphal and larval ticks as compared to years with lower temperatures. Model predictions suggest up to a two-week average earlier activity period for larvae and nymphs if 2050 warming predictions hold (Levi et al. 2015), which provide additional opportunity for overlap with humans and domestic animals. Given that the risk of acquiring a tickborne illness like Lyme disease is heavily dependent on not only the enzootic cycle of disease, but also on human behavior, our predictions can help identify areas of Illinois to concentrate additional surveillance efforts to more accurately quantify that acarological risk. Predicted *A. americanum* habitat for the historical climate closely matches reported occurrence within Illinois (IDPH 2022). Currently this species is most abundant in the southern portion of the state but is becoming increasingly more common in the north (Ma et al. 2021; Rochlin et al. 2022; Fowler et al. 2022). *A. americanum*'s aggressive host seeking and non-specific host preferences create an optimal dispersal scenario which allow this tick to travel long distances on meso-mammals and deer, as well as birds (Goddard and Varella-Stokes 2009).

However, *D. variabilis* and *A. americanum* were also found to be constrained by the 2070 climate scenarios in similar habitats but were more likely to occur throughout more of the forested southern portion of the state, like previous research (Oliveira et al. 2017). *A. maculatum* was the only tick predicted to continue to expand throughout the state as the temperatures rose more extremely into the 2070 climate. Of greatest concern for public health is the increasing likelihood of these additional vector tick species near the higher population centers along the Illinois River and surrounding Chicago. We have found that few medical professionals in northern areas in Illinois were familiar with the risk of ehrlichiosis within the state (Carson 2022), despite 422 cases between 2011 and 2021 (IDPH 2022). This is likely due to the current abundance of *A. americanum* being higher in the southern portion of the state and is likely to delay diagnosis and treatment of pathogens vectored by these less-studied tick species. Both Bayles et al. (2013) and Soucy & de Urioste-Stone (2020) also found that adoption of effective tick prevention measures, such as tick checks, was associated with perceived risk of tick bites. As actual risk of tick exposure changes due to shifting tick habitat and abundance, public and professional awareness must be addressed through dynamic communication efforts.

We focused on more extreme expectations for future climate scenarios to capture a likely "worst case scenario" for future tickborne disease risk, mainly because the entirety of Illinois is expected to be within a projected "extreme heat belt" with heat index temperatures exceeding 125 degrees Fahrenheit for at least one day by 2053 (First Street

 doi:10.20944/preprints202211.0490.v1

Foundation 2022). Broader studies that have examined potential tick niche expansion and retraction under future scenarios have found similar results for these species regardless of the global circulation model chosen. Ma et al. (2022) explored the impact of several shared socioeconomic pathways through 2100 and predicted all of Illinois to be highly suitable for *A. americanum* during all scenarios ranging from least impactful to most impactful. These projections combine climate model data with policy to best capture a likely outcome for climate change. Employing ecological niche models with RCP 4.5 and RCP 8.5 predicted a similar suitability outcome for *A. americanum* in North America (Raghavan et al. 2016, 2019), as did a study by Boorgula et al. (2020) which predicted moderate to high suitability for *D. variabilis* throughout the state continued through both RCP 4.5 and RCP 8.5 scenarios. While Flenniken et al. (2022) did not examine future projections of *A. maculatum*, they found that under current climate conditions the expected ecological niche for this species is much greater than its current distribution, suggesting the potential for expansion north and east. By focusing on Illinois alone, we were able to apply a more fine-scale environmental niche prediction for each of these four tick species within the RCP 4.5 and 8.5 scenarios.

We recognize several limitations in our investigation. It is important to note that species distribution modelling is often subject to confounding due to the phenomenological approach to predicting tick distributions. Spurious correlations can be assumed without additional mechanistic understanding of the relationships among ticks and these environmental predictors at a smaller scale (Ostfeld & Brunner 2015). We attempted to control for this, in part, by including known white-tailed deer habitat, but this variable was removed due to collinearity issues with other environmental correlates. Previous work also demonstrated that for certain species, like *I. scapularis*, tick presence varied despite host availability, suggesting a more influential role of abiotic variables (Guerra et al. 2002). While the inclusion of other forest-level habitat variables likely replaced the need for specific deer habitat, we consider it a limitation given the need for and importance of considering reproductive host species in habitat models. However, in the case of the Lyme bacteria (*Borrelia burgdorferi*) recent evidence may suggest that overall tickborne disease hazard risk posed by the positive association between deer density and nymphal tick density is cancelled out through opposing forces of both amplification and dilution since deer are not a competent reservoir for the bacteria (Gandy et al. 2022).

Our environmental correlates included climate variables that change according to proposed scenarios, but the landcover predictors did not include estimates of variability. As landcover predictors did not change over time, our model results therefore assume that the changes in climate do not change the percentage of cropland or other landcover types throughout the state. ESRI landscape change predictions for 2050 in Illinois included an expected gain of over 821,000 acres of cropland throughout the state, a gain of over 503,000 acres of developed or impervious surface, and losses of deciduous forest (743,000 acres), grassland (380,000 acres), and wetland (39,224 acres) (ESRI Landcover 2050). Future modeling work should include these predictions to improve upon static landscape assumptions. Further, the historical climate and landscape variables were slightly mismatched (climate was a mean from 1970-2000, whereas the landscape mean ranged

 doi:10.20944/preprints202211.0490.v1

from 2001-2016). These differences could potentially impact the model accuracy. We did not incorporate soil types or profiles (Guerra et al. 2002) into the models which also may have impacted the predictions due to their ability to harbor and control microclimates and habitats that can impact tick survival. However, since only certain vegetation is expected to grow according to various soil profiles (Guerra et al. 2002), we assumed that vegetation was enough of a proxy for these models.

Booth (2022) reported that certain combined temperature and precipitation bioclimatic variables can be unreliable in species distribution modeling depending on proximity to the equator due to discontinuities in interpolation and can result in extreme differences over short distances. In the United States, specifically, mean temperature of the warmest quarter (bio8), and mean temperature of the driest quarter (bio9) demonstrated anomalies in the south and southeastern regions of the country (Booth 2022). These discontinuities were like others that occurred globally near the equator. These anomalies should not have impacted our results because of Illinois' distance from the equator, but mention is warranted since these variables were important in our models.

Sampling bias consideration is important with occurrence data and may have influence potentially seen in response curves of *I. scapularis* in the historical climate. Previous research (Diuk-Wasser et al. 2021) showed an increasing likelihood of presence of *I. scapularis* in uninterrupted forest, whereas our results demonstrate a large decline in the likelihood of *I. scapularis* occurrence with increasing percentage of forest cover. This could reflect a lack of data points collected from deeper within forests (i.e. collections intentionally performed in easily accessible places because this is where the disease transmission risk is), or that this species spends more time in edge environments within Illinois. The sampling method (drag versus CO2 trap versus small animal capture) is also important to consider when assessing bias. Rynkiewicz et al. (2014) reported that *I. scapularis* was mainly found collected from small mammals while *A. americanum* and *D. variabilis* were able to be collected using cloth drag and CO2 protocols. Records of *I. scapularis* in Illinois may therefore be underrepresented, as most sampling in the state has used the cloth drag approach.

The very small data set for *A. maculatum* may have contributed to projected future results suggesting a lack of *A. maculatum* in landscapes that it is known to thrive in, like grasslands, or future projections associating the tick with croplands. Specifically, the sample size may have impacted the accuracy of the random forest/CART predictions per class overlap as previously stated (Valavi et al. 2021). Reevaluation of this tick's expected distribution as more data become available is necessary.

5. Conclusions

The variable landscape of Illinois creates a patchwork of risk to humans and domestic animals that can be predicted based on climate and landscape features. As the climate changes over the coming decades, the distribution of these tick species will change as it adapts to the increasing temperatures. Knowing where ticks may concentrate will be important to anticipating, preventing, and treating tickborne disease.

 doi:10.20944/preprints202211.0490.v1

Supplementary Materials: The following supporting information can be downloaded at: www.mdpi.com/xxx/s1, Figures S1 – S8.

Author Contributions:

HLK: Conceptualization, Data curation, Investigation, Formal analysis, Writing – original draft, Writing – review and editing

PG: Visualization, Writing – review and editing

NMP: Conceptualization, Writing – original draft, Writing – review and editing

RLS: Conceptualization, Supervision, Funding acquisition, Writing – original draft, Writing – review and editing

Funding: This work was supported by the Department of Defense grant number: TB180052.

Data Availability Statement: Data and code can be accessed here: https://github.com/hkop-sco/ILTickSDM

Acknowledgments: We are grateful to all the researchers who cataloged, contributed, and maintained tick occurrence observations in public data bases.

Conflicts of Interest: The authors declare no conflict of interest.

References

6th National Risk Assessment of Hazardous Heat [WWW Document], n.d.. FirstStreet. URL https://firststreet.org/research-lab/published-research/article-highlights-from-hazardous-heat/ (accessed 11.12.22).

Aiello-Lammens, M.E., Boria, R.A., Radosavljevic, A., Vilela, B., Anderson, R.P., 2015. spThin: an R package for spatial thinning of species occurrence records for use in ecological niche models. Ecography 38, 541–545. https://doi.org/10.1111/ecog.01132

Allan, B.F., Keesing, F., Ostfeld, R.S., 2003. Effect Of Forest Fragmentation on Lyme Disease Risk. Conserv. Biol. 17, 267–272. https://doi.org/10.1046/j.1523-1739.2003.01260.x

Alkishe, A., Raghavan, R.K., Peterson, A.T., 2021. Likely Geographic Distributional Shifts among Medically Important Tick Species and Tick-Associated Diseases under Climate Change in North America: A Review. Insects 12. https://doi.org/10.3390/insects12030225

Alkishe, A., Peterson, A.T., 2022. Climate change influences on the geographic distributional potential of the spotted fever vectors *Amblyomma maculatum* and *Dermacentor andersoni*. PeerJ 10, e13279. https://doi.org/10.7717/peerj.13279

Allouche, O., Tsoar, A., Kadmon, R., 2006. Assessing the accuracy of species distribution models: prevalence, kappa and the true skill statistic (TSS). J. Appl. Ecol. 43, 1223–1232. https://doi.org/10.1111/j.1365-2664.2006.01214.x

Bacon, E.A., Kopsco, H., Gronemeyer, P., Mateus-Pinilla, N., Smith, R.L., 2022. Effects of Climate on the Variation in Abundance of Three Tick Species in Illinois. J. Med. Entomol. 59, 700–709. https://doi.org/10.1093/jme/tjab189

Barbet-Massin, M., Jiguet, F., Albert, C.H., Thuiller, W., 2012. Selecting pseudo-absences for species distribution models: how, where and how many? Methods Ecol. Evol. 3, 327–338. https://doi.org/10.1111/j.2041-210x.2011.00172.x

Bayles, B.R., Evans, G., Allan, B.F., 2013. Knowledge and prevention of tick-borne diseases vary across an urban-to-rural human land-use gradient. Ticks Tick Borne Dis. 4, 352–358. https://doi.org/10.1016/j.ttbdis.2013.01.001

Berger, K.A., Ginsberg, H.S., Gonzalez, L., Mather, T.N., 2014a. Relative humidity and activity patterns of Ixodes scapularis (Acari: Ixodidae). J. Med. Entomol. 51, 769–776. https://doi.org/10.1603/me13186

Berger, K.A., Ginsberg, H.S., Dugas, K.D., Hamel, L.H., Mather, T.N., 2014b. Adverse moisture events predict seasonal abundance of Lyme disease vector ticks (Ixodes scapularis). Parasites and Vectors 7, 1–8. https://doi.org/10.1186/1756-3305-7-181

Boorgula, G.D.Y., Peterson, A.T., Foley, D.H., Ganta, R.R., Raghavan, R.K., 2020. Assessing the current and future potential geographic distribution of the American dog tick, Dermacentor variabilis (Say) (Acari: Ixodidae) in North America. PLoS One 15, e0237191. https://doi.org/10.1371/journal.pone.0237191

Booth, T.H., 2022. Checking bioclimatic variables that combine temperature and precipitation data before their use in species distribution models. Austral Ecol. https://doi.org/10.1111/aec.13234

Brownstein, J.S., Holford, T.R., Fish, D., 2005. Effect of Climate Change on Lyme Disease Risk in North America. Ecohealth 2, 38–46. https://doi.org/10.1007/s10393-004-0139-x

Carson, D.A., Kopsco, H., Gronemeyer, P., Mateus-Pinilla, N., Smith, G.S., Sandstrom, E.N., Smith, R.L., 2022. Knowledge, attitudes, and practices of Illinois medical professionals related to ticks and tick-borne disease. One Health 15, 100424. https://doi.org/10.1016/j.onehlt.2022.100424

Diuk-Wasser, M.A., VanAcker, M.C., Fernandez, M.P., 2021. Impact of Land Use Changes and Habitat Fragmentation on the Eco-epidemiology of Tick-Borne Diseases. J. Med. Entomol. 58, 1546–1564. https://doi.org/10.1093/jme/tjaa209

Drake, J.M., Randin, C., Guisan, A., 2006. Modelling ecological niches with support vector machines. J. Appl. Ecol. 43, 424–432. https://doi.org/10.1111/j.1365-2664.2006.01141.x

Ferrell, A.M., Brinkerhoff, R.J., 2018. Using landscape analysis to test hypotheses about drivers of tick abundance and infection prevalence with Borrelia burgdorferi. Int. J. Environ. Res. Public Health 15, 18–20. https://doi.org/10.3390/ijerph15040737

Flenniken, J.M., Tuten, H.C., Rose Vineer, H., Phillips, V.C., Stone, C.M., Allan, B.F., 2022. Environmental Drivers of Gulf Coast Tick (Acari: Ixodidae) Range Expansion in the United States. J. Med. Entomol. https://doi.org/10.1093/jme/tjac091

Fowler, P.D., Nguyentran, S., Quatroche, L., Porter, M.L., Kobbekaduwa, V., Tippin, S., Miller, G., Dinh, E., Foster, E., Tsao, J.I., 2022. Northward Expansion of Amblyomma americanum (Acari: Ixodidae) into Southwestern Michigan. J. Med. Entomol. https://doi.org/10.1093/jme/tjac082

Gandy, S., Kilbride, E., Biek, R., Millins, C., Gilbert, L., 2022. No net effect of host density on tick-borne disease hazard due to opposing roles of vector amplification and pathogen dilution. Ecol. Evol. 12. https://doi.org/10.1002/ece3.9253

Gilliam, B., Gronemeyer, P., Chakraborty, S., Winata, F., Lyons, L.A., Miller-Hunt, C., Tuten, H.C., Debosik, S., Freeman, D., O'hara-Ruiz, M., Mateus-Pinilla, N., 2020. Impact of Unexplored Data Sources on the Historical Distribution of Three Vector Tick Species in Illinois. J. Med. Entomol. 57, 872–883. https://doi.org/10.1093/jme/tjz235

Grimmett, L., Whitsed, R., Horta, A., 2020. Presence-only species distribution models are sensitive to sample prevalence: Evaluating models using spatial prediction stability and accuracy metrics. Ecol. Modell. 431, 109194. https://doi.org/10.1016/j.ecolmodel.2020.109194

Guerra, M.A., Walker, E.D., Kitron, U., 2001. Canine surveillance system for Lyme borreliosis in Wisconsin and northern Illinois: geographic distribution and risk factor analysis. Am. J. Trop. Med. Hyg. 65, 546–552. https://doi.org/10.4269/ajtmh.2001.65.546

Guerra, M., Walker, E., Jones, C., Paskewitz, S., Cortinas, M.R., Stancil, A., Beck, L., Bobo, M., Kitron, U., 2002. Predicting the risk of Lyme disease: habitat suitability for Ixodes scapularis in the north central United States. Emerg. Infect. Dis. 8, 289–297. https://doi.org/10.3201/eid0803.010166

Heske, E.J., 1995. Mammalian Abundances on Forest-Farm Edges versus Forest Interiors in Southern Illinois: Is There an Edge Effect? J. Mammal. 76, 562–568. https://doi.org/10.2307/1382364

Hijmans R.J. (2022). raster: Geographic Data Analysis and Modeling. R package version 3.5-15. https://CRAN.R-project.org/package=raster

Hook, S.A., Jeon, S., Niesobecki, S.A., Hansen, A.P., Meek, J.I., Bjork, J.K.H., Dorr, F.M., Rutz, H.J., Feldman, K.A., White, J.L., Backenson, P.B., Shankar, M.B., Meltzer, M.I., Hinckley, A.F., 2022. Economic Burden of Reported Lyme Disease in High-Incidence Areas, United States, 2014-2016. Emerg. Infect. Dis. 28, 1170–1179. https://doi.org/10.3201/eid2806.211335

Illinois Department of Public Health. 2017a. Reportable Communicable Disease Cases, 1990 - 1999 - data.illinois.gov [WWW Document], n.d. URL https://data.illinois.gov/dataset/633reportable_communicable_disease_cases_1990_1999 (accessed 7.27.22).

Illinois Department of Public Health. 2017b. Reportable Communicable Disease Cases, 2000 - 2009 - data.illinois.gov [WWW Document], n.d. URL https://data.illinois.gov/dataset/634reportable_communicable_disease_cases_2000_2009 (accessed 7.27.22).

Illinois Department of Public Health. 2018. Reportable Communicable Disease Cases, 2010 - 2017 - data.illinois.gov [WWW Document], n.d. URL https://data.illinois.gov/dataset/635reportable_communicable_disease_cases_2010_2012 (accessed 7.27.22).

Illinois Department of Public Health. 2022. Story Map Series [WWW Document], n.d. URL https://idph.maps.arcgis.com/apps/MapSeries/index.html?appid=976061db733441eb977ef5cf2facd5c4 (accessed 11.1.22).

Illinois Department of Public Health. 2022. Reported Tickborne Cases 2011-2021 [WWW Document], n.d. URL https://dph.illinois.gov/topics-services/diseases-and-conditions/diseases-a-z-list/lyme-disease/data/tickborne-cases-2011-2021.html (accessed 11.8.22).

Jin, S., Homer, C., Yang, L., Danielson, P., Dewitz, J., Li, C., Zhu, Z., Xian, G., Howard, D., 2019. Overall Methodology Design for the United States National Land Cover Database 2016 Products. Remote Sensing 11, 2971. https://doi.org/10.3390/rs11242971 Jobe, D.A., Nelson, J.A., Adam, M.D., Martin, S.A., Jr, 2007. Lyme disease in urban areas, Chicago. Emerg. Infect. Dis. 13, 1799–1800. https://doi.org/10.3201/eid1311.070801

Johnson, D.K.H., Schiffman, E.K., Davis, J.P., Neitzel, D.F., Sloan, L.M., Nicholson, W.L., Fritsche, T.R., Steward, C.R., Ray, J.A., Miller, T.K., Feist, M.A., Uphoff, T.S., Franson, J.J., Livermore, A.L., Deedon, A.K., Theel, E.S., Pritt, B.S., 2015. Human Infection with Ehrlichia muris-like Pathogen, United States, 2007-2013(1). Emerg. Infect. Dis. 21, 1794–1799. https://doi.org/10.3201/eid2110.150143

Kilpatrick, A.M., Dobson, A.D.M., Levi, T., Salkeld, D.J., Swei, A., Ginsberg, H.S., Kjemtrup, A., Padgett, K.A., Jensen, P.M., Fish, D., Ogden, N.H., Diuk-Wasser, M.A., 2017. Lyme disease ecology in a changing world: consensus, uncertainty and critical gaps for improving control. Philos. Trans. R. Soc. Lond. B Biol. Sci. 372. https://doi.org/10.1098/rstb.2016.0117

Kopsco, H.L., Duhaime, R.J., Mather, T.N., 2021. Crowdsourced Tick Image-Informed Updates to U.S. County Records of Three Medically Important Tick Species. J. Med. Entomol. 58, 2412–2424. https://doi.org/10.1093/jme/tjab082

Kopsco, H.L., Smith, R.L., Halsey, S.J., 2022. A Scoping Review of Species Distribution Modeling Methods for Tick Vectors. Frontiers in Ecology and Evolution 10. https://doi.org/10.3389/fevo.2022.893016

Levi, T., Keesing, F., Oggenfuss, K., Ostfeld, R.S., 2015. Accelerated phenology of blacklegged ticks under climate warming. Philos. Trans. R. Soc. Lond. B Biol. Sci. 370. https://doi.org/10.1098/rstb.2013.0556

Lewis, S., 2013. ACCESS1-0 climate model output prepared for the Coupled Model Intercomparison Project Phase 5 (CMIP5) historical experiment, r2i1p1 ensemble. https://doi.org/10.1594/WDCC/CMIP5.CSA0hi

Lippi, C.A., Gaff, H.D., White, A.L., Ryan, S.J., 2021a. Scoping review of distribution models for selected Amblyomma ticks and rickettsial group pathogens. PeerJ 9, e10596. https://doi.org/10.7717/peerj.10596

Lippi, C.A., Gaff, H.D., White, A.L., St John, H.K., Richards, A.L., Ryan, S.J., 2021b. Exploring the Niche of Rickettsia montanensis (Rickettsiales: Rickettsiaceae) Infection of the American Dog Tick (Acari: Ixodidae), Using Multiple Species Distribution Model Approaches. J. Med. Entomol. 58, 1083–1092. https://doi.org/10.1093/jme/tjaa263

Lockwood, B.H., Stasiak, I., Pfaff, M.A., Cleveland, C.A., Yabsley, M.J., 2018. Widespread distribution of ticks and selected tick-borne pathogens in Kentucky (USA). Ticks Tick Borne Dis. 9, 738–741. https://doi.org/10.1016/j.ttbdis.2018.02.016

Lyons, L.A., Brand, M.E., Gronemeyer, P., Mateus-Pinilla, N., Ruiz, M.O., Stone, C.M., Tuten, H.C., Smith, R.L., 2021. Comparing Contributions of Passive and Active Tick Collection Methods to Determine Establishment of Ticks of Public Health Concern Within Illinois. J. Med. Entomol. https://doi.org/10.1093/jme/tjab031

Ma, D., Lun, X., Li, C., Zhou, R., Zhao, Z., Wang, J., Zhang, Q., Liu, Q., 2021. Predicting the Potential Global Distribution of *Amblyomma americanum* (Acari: Ixodidae) under Near Current and Future Climatic Conditions, Using the Maximum Entropy Model. Biology 10. https://doi.org/10.3390/biology10101057

Martin, J.T., Fischhoff, I.R., Castellanos, A.A., Han, B.A., 2022. Ecological Predictors of Zoonotic Vector Status Among Dermacentor Ticks (Acari: Ixodidae): A Trait-Based Approach. J. Med. Entomol. https://doi.org/10.1093/jme/tjac125

McBride, S.E., Lieberthal, B.A., Buttke, D.E., Cronk, B.D., De Urioste-Stone, S.M., Goodman, L.B., Guarnieri, L.D., Rounsville, T.F., Gardner, A.M., 2022. Patterns and Ecological Mechanisms of Tick-Borne Disease Exposure Risk in Acadia National Park, Mount Desert Island, Maine, United States. J. Med. Entomol. https://doi.org/10.1093/jme/tjac152

Molaei, G., Eisen, L.M., Price, K.J., Eisen, R.J., 2022. Range Expansion of Native and Invasive Ticks, a Looming Public Health Threat. J. Infect. Dis. https://doi.org/10.1093/infdis/jiac249

Naimi, B., Araújo, M.B., 2016. sdm: a reproducible and extensible R platform for species distribution modelling. Ecography 39, 368–375. https://doi.org/10.1111/ecog.01881

Naimi, B., Araújo, M.B., 2016. Package "sdm." cran.r-project.org › web › packages › sdm › sdmcran.r-project.org › web › packages › sdm › sdm.

Noden, B.H., Dubie, T., 2017. Involvement of invasive eastern red cedar (*Juniperus virginiana*) in the expansion of *Amblyomma americanum* in Oklahoma. J. Vector Ecol. 42, 178–183. https://doi.org/10.1111/jvec.12253

Ogden, N.H., Radojevic, M., Wu, X., Duvvuri, V.R., Leighton, P.A., Wu, J., 2014. Estimated effects of projected climate change on the basic reproductive number of the Lyme disease vector Ixodes scapularis. Environ. Health Perspect. 122, 631–638. https://doi.org/10.1289/ehp.1307799

Ogden, N.H., Ben Beard, C., Ginsberg, H.S., Tsao, J.I., 2020. Possible Effects of Climate Change on Ixodid Ticks and the Pathogens They Transmit: Predictions and Observations. J. Med. Entomol. https://doi.org/10.1093/jme/tjaa220

Oliveira, S.V. de, Romero-Alvarez, D., Martins, T.F., Santos, J.P. dos, Labruna, M.B., Gazeta, G.S., Escobar, L.E., Gurgel-Gonçalves, R., 2017. Amblyomma ticks and future climate: Range contraction due to climate warming. Acta Trop. 176, 340–348. https://doi.org/10.1016/j.actatropica.2017.07.033

Ostfeld, R.S., Brunner, J.L., 2015. Climate change and Ixodes tick-borne diseases of humans. Philos. Trans. R. Soc. Lond. B Biol. Sci. 370, 20140051–. https://doi.org/10.1098/rstb.2014.0051

Paddock, C.D., Goddard, J., 2015. The Evolving Medical and Veterinary Importance of the Gulf Coast tick (Acari: Ixodidae). J. Med. Entomol. 52, 230–252. https://doi.org/10.1093/jme/tju022

Pascoe, E. L., Marcantonio, M., Caminade, C., and Foley, J. E. (2019). Modeling Potential Habitat for Amblyomma Tick Species in California. *Insects* 10, 201. doi:10.3390/insects10070201.

Phillips, V.C., Zieman, E.A., Kim, C.-H., Stone, C.M., Tuten, H.C., Jiménez, F.A., 2020. Documentation of the Expansion of the Gulf Coast Tick (Amblyomma maculatum) and Rickettsia parkeri: First Report in Illinois. J. Parasitol. 106, 9–13.

Raghavan, R.K., Goodin, D.G., Hanzlicek, G.A., Zolnerowich, G., Dryden, M.W., Anderson, G.A., Ganta, R.R., 2016. Maximum Entropy-Based Ecological Niche Model and Bio-Climatic Determinants of Lone Star Tick (Amblyomma americanum) Niche. Vector Borne Zoonotic Dis. 16, 205–211. https://doi.org/10.1089/vbz.2015.1837

Raghavan, R.K., Peterson, A.T., Cobos, M.E., Ganta, R., Foley, D., 2019. Current and Future Distribution of the Lone Star Tick, Amblyomma americanum (L.) (Acari: Ixodidae) in North America. PLoS One 14, e0209082. https://doi.org/10.1371/journal.pone.0209082

Raghavan, R.K., Koestel, Z.L., Boorgula, G., Hroobi, A., Ganta, R., Harrington, J., Jr, Goodin, D., Stich, R.W., Anderson, G., 2021. Unexpected winter questing activity of ticks in the Central Midwestern United States. PLoS One 16, e0259769. https://doi.org/10.1371/journal.pone.0259769

Randolph, S.E., Storey, K., 1999. Impact of microclimate on immature tick-rodent host interactions (Acari: Ixodidae): implications for parasite transmission. J. Med. Entomol. 36, 741–748. https://doi.org/10.1093/jmedent/36.6.741

Riahi, K., Rao, S., Krey, V., Cho, C., Chirkov, V., Fischer, G., Kindermann, G., Nakicenovic, N., Rafaj, P., 2011. RCP 8.5—A scenario of comparatively high greenhouse gas emissions. Clim. Change 109, 33. https://doi.org/10.1007/s10584-011-0149-y

Robinson, S.J., Neitzel, D.F., Moen, R.A., Craft, M.E., Hamilton, K.E., Johnson, L.B., Mulla, D.J., Munderloh, U.G., Redig, P.T., Smith, K.E., Turner, C.L., Umber, J.K., Pelican, K.M., 2015. Disease Risk in a Dynamic Environment: The Spread of Tick-Borne Pathogens in Minnesota, USA. Ecohealth 12, 152–163. https://doi.org/10.1007/s10393-014-0979-y

Rochlin, I., 2019. Modeling the Asian Longhorned Tick (Acari: Ixodidae) Suitable Habitat in North America. J. Med. Entomol. 56, 384–391. https://doi.org/10.1093/jme/tjy210

Rochlin, I., Egizi, A., Lindström, A., 2022. The original scientific description of the Lone Star tick (Amblyomma americanum, Acari: Ixodidae) and implications for the species' past and future geographic distributions. J. Med. Entomol. 59, 412–420. https://doi.org/10.1093/jme/tjab215

Rydzewski, J., Mateus-Pinilla, N., Warner, R.E., Hamer, S., Weng, H.-Y., 2011. Ixodes scapularis and Borrelia burgdorferi among diverse habitats within a natural area in east-central Illinois. Vector Borne Zoonotic Dis. 11, 1351–1358. https://doi.org/10.1089/vbz.2010.0160

Rynkiewicz, E.C., Clay, K., 2014. Tick community composition in Midwestern US habitats in relation to sampling method and environmental conditions. Exp. Appl. Acarol. 64, 109–119. https://doi.org/10.1007/s10493-014-9798-7

Savage, H.M., Burkhalter, K.L., Godsey, M.S., Jr, Panella, N.A., Ashley, D.C., Nicholson, W.L., Lambert, A.J., 2017. Bourbon virus in field-collected ticks, Missouri, USA. Emerg. Infect. Dis. 23, 2017–2022. https://doi.org/10.3201/eid2312.170532

Sonenshine, D.E., 2018. Range Expansion of Tick Disease Vectors in North America: Implications for Spread of Tick-Borne Disease. Int. J. Environ. Res. Public Health 15. https://doi.org/10.3390/ijerph15030478

Soucy, A., de Urioste-Stone, S., 2020. TOURIST BEHAVIOUR AND TICK-BORNE DISEASE RISK, in: WIT Transactions on Ecology and the Environment. WIT Press, pp. 77–88. https://doi.org/10.2495/ST200071

Springer, Y.P., Eisen, L., Beati, L., James, A.M., Eisen, R.J., 2014. Spatial Distribution of Counties in the Continental United States With Records of Occurrence of Amblyomma americanum (Ixodida: Ixodidae). J. Med. Entomol. 51, 342–351. https://doi.org/10.1603/ME13115

Strobl, C., Malley, J., Tutz, G., 2009. An introduction to recursive partitioning: rationale, application, and characteristics of classification and regression trees, bagging, and random forests. Psychol. Methods 14, 323–348. https://doi.org/10.1037/a0016973

Tuten, H.C., Burkhalter, K.L., Noel, K.R., Hernandez, E.J., Yates, S., Wojnowski, K., Hartleb, J., Debosik, S., Holmes, A., Stone, C.M., 2020. Heartland Virus in Humans and Ticks, Illinois, USA, 2018-2019. Emerg. Infect. Dis. 26, 1548–1552. https://doi.org/10.3201/eid2607.200110

U.S. Geological Survey (USGS) - Gap Analysis Project (GAP), 2018, White-tailed Deer (*Odocoileus virginianus*) mWTDEx_CONUS_2001v1 Habitat Map: U.S. Geological Survey data release, https://doi.org/10.5066/F7SF2TM0.

Valavi, R., Elith, J., Lahoz-Monfort, J.J., Guillera-Arroita, G., 2021. Modelling species presence-only data with random forests. Ecography 44, 1731–1742. https://doi.org/10.1111/ecog.05615

Valavi, R., Guillera-Arroita, G., Lahoz-Monfort, J.J., Elith, J., 2022. Predictive performance of presence-only species distribution models: a benchmark study with reproducible code. Ecol. Monogr. 92. https://doi.org/10.1002/ecm.1486

Wikel, S.K., 2022. Changing Geographic Ranges of Human Biting Ticks and Implications for Tick-Borne Zoonoses in North America. Zoonotic Diseases 2, 126–146. https://doi.org/10.3390/zoonoticdis2030013

Yang, L., Jin, S., Danielson, P., Homer, C., Gass, L., Case, A., Costello, C., Dewitz, J., Fry, J., Funk, M., Grannemann, B., Rigge, M. and G. Xian. 2018. A New Generation of the United States National Land Cover Database: Requirements, Research Priorities, Design, and Implementation Strategies, ISPRS Journal of Photogrammetry and Remote Sensing, 146, pp.108-123.